NBSIR 75-742

Mixed Oxides for Fuel Cell Electrodes

U. Bertocci, M. I. Cohen, W. S. Horton, T. Negas, and A. R. Siedle

Institute for Materials Research
National Bureau of Standards
Washington, D. C. 20234

January 1976

Final Report

Prepared for

Industrial Environmental Research Laboratory
Office of Research and Development
U.S. Environmental Protection Agency
Research Triangle Park, North Carolina 27711

NBSIR 75-742

MIXED OXIDES FOR FUEL CELL ELECTRODES

U. Bertocci, M. I. Cohen, W. S. Horton, T. Negas, and A. R. Siedle

Institute for Materials Research
National Bureau of Standards
Washington, D. C. 20234

January 1976

Final Report

Prepared for
Industrial Environmental Research Laboratory
Office of Research and Development
U.S. Environmental Protection Agency
Research Triangle Park, North Carolina 27711

U.S. DEPARTMENT OF COMMERCE, Rogers C.B. Morton, *Secretary*
James A. Baker, III, *Under Secretary*
Dr. Betsy Ancker-Johnson, *Assistant Secretary for Science and Technology*

NATIONAL BUREAU OF STANDARDS, Ernest Ambler, *Acting Director*

ABSTRACT

This report presents studies of the preparation, chemical stability, and electrochemical behavior of mixed oxides in order to determine if these are potential candidates as oxygen-reducing electrocatalysts in an acid fuel cell. Materials studied included strontium and barium cobaltates and manganates with and without added titanium; lanthanum titanates, with and without calcium or strontium; calcium, strontium, and barium ruthenates; and mixed oxides of the systems Ti-Ta-O, V-Nb-O, Ce-Ta-O, Pr-Ta-O, Ce-Nb-O, and Ce-Pr-Ta-O. The choices were based upon producing variable valence for a given transition metal and upon conferring stability at elevated temperatures ($\lesssim$ 150 °C) in phosphoric acid using oxides of known stability. Barium ruthenate and the systems Ti-Ta-O, V-Nb-O, V-Ta-O, Ce-Ta-O were hot-acid stable. The high temperature reactions of $CeTaO_{4+x}$ with $0 \lesssim x \lesssim 0.5$ were studied in air up to about 1960 °C.

Potentiodynamic and galvanostatic studies are reported for materials from the Ti-Ta-O system, TiO_2 as grown, TiO_2 reduced with hydrogen, TiO_2 with 0.1% Nb, lanthanum titanates with and without calcium or strontium, a tungsten bronze, barium ruthenate, and strontium titanate with 0.03% and with 0.15% Nb.

Because the reduction of oxygen is easier than that of nitrogen, and because biochemical reduction of nitrogen takes place rather easily, preparation of inorganic compounds with ternary metal-sulfur arrays similar to the arrays in nitrogen reductase was attempted. These compounds were also to be tested in a manner similar to the mixed oxides. The following were made: $(Ph_3P)_4Cu_2W_2S_6$, $(Ph_3P)_6Ag_5W_2S_6O_2$, and $[(Ph_3P)_3Ag]_2W_2S_6$, where Ph_3P refers to the triphenylphosphine moiety. Also prepared were $(Ph_3PAu)_2W_2S_4$, $(Ph_3AsAu)_2WS_4$, $(diphos)NiWO_2S_2$, $(diphos)_2Pd_3W_2S_6O_2$, and $(Ph_3P)_3PtW_2S_6O_2$, where "diphos" refers to 1,2-bis(diphenylphosphino)ethane.

TABLE OF CONTENTS

		Page
Abstract		ii
List of Figures		v
Acknowledgements		vi
I.	CONCLUSIONS	1
II.	RECOMMENDATIONS	2
III.	INTRODUCTION	3
	General	3
	Objectives	4
	Sections	4
IV.	ACID STABILITY	6
	Method of Test	6
	Results	7
V.	PHASE STUDIES AND MATERIALS PREPARATION	9
VI.	ELECTROCHEMICAL MEASUREMENTS	16
	Introduction	16
	Experimental Arrangement	16
	Description of Experimental Set-up	16
	Description of Cells Used	16
	Electrodes	18
	Experimental Methods	23
	Potentiodynamic Measurements	23
	Titanates	23
	Tungsten Bronze	26
	Barium Ruthenate	26
	Redox Measurements	33
	Titanates	33
	Tungsten Bronze	34
	Barium Ruthenate	35
	Discussion	39

Page

VII. MATERIALS OTHER THAN OXIDES 42

Introduction 42

Results 42

Aqueous Systems 42

Nonaqueous Systems 43

VIII. REFERENCES 46

IX. LIST OF PUBLICATIONS 48

LIST OF FIGURES

1. Block diagram of electrochemical instrumentation. Page 17.
2. Electrochemical cell used at room temperature with Type I electrode. Page 19.
3. Type II electrode shown in front view and cross-section. Page 21.
4. Current-potential curve for $95TiO_2:5Ta_2O_5$ in 5 mol/l H_3PO_4 at room temperature. Page 24.
5. Current-potential curves for the lanthanum titanates at room temperature. Page 25.
6. Current-potential curves for a Type II $BaRuO_3$ electrode in concentrated phosphoric acid at 60 °C. Page.27.
7. Effect of oxygen and the current-potential curve for a Type II $BaRuO_3$ electrode. Page 29.
8. Current-potential curve for a Type II $BaRuO_3$ electrode in neutral solution. Page 30.
9. Comparison of two $BaRuO_3$ electrodes (Type II) in 6 mol/l NaOH at 60 °C. Page 31.
10. The effect of 0.007M H_2O_2 on a Type II $BaRuO_3$ and on smooth Pt. Page 32.
11. Steady-state performance of Type II $BaRuO_3$ electrode with ferro-ferricyanide reaction; semilog scale. Page 36.
12. Steady-state performance of Type II $BaRuO_3$ electrode with ferro-ferricyanide reaction; linear scale. Page 37.
13. Steady-state performance of Type II $BaRuO_3$ electrode with iodine-iodide reaction. Page 38.

ACKNOWLEDGEMENTS

The work reported herein was performed by Dr. U. Bertocci, Mr. M. I. Cohen, Dr. T. Negas, and Dr. A. R. Siedle, with the assistance of Mr. N. K. Adams, Mr. J. L. Mullen, Mr. C. D. Olson, and Mr. J. Broussalian.

Dr. A. D. Franklin provided overall scientific guidance. Dr. H. P. R. Frederikse participated constructively in a number of the discussions particularly those dealing with catalytic effects of a variety of perovskites. Dr. R. S. Roth provided valuable crystallographic data and advice on the cerium tantalates and the metal thiotungstate derivatives. Mr. H. S. Parker gave valuable assistance with preparation of single crystals. Dr. G. A. Candela performed and interpreted magnetic measurements. All of the above collaborators are at NBS.

Mr. N. L. Loeffler, University of Tennessee, engendered the interest in and collaborated in the preparation of the lanthanum titanates.

SECTION I

CONCLUSIONS

On the basis of consideration of stoichiometry and the expected effect on electron transport properties, the mixed oxides containing rare earths (cesium and/or praeseodymium) and certain transition metals (titanium, vanadium, niobium, and tantalum) may be quite interesting as candidates for electrocatalytic applications in hot-acid fuel cells. It has been shown that some are stable in hot, concentrated phosphoric acid. The high temperature phase relations important to their preparation have been studied.

Barium ruthenate, although exhibiting stability in hot, phosphoric acid, appeared to change chemically during the passage of electric current. This material may not be useful as a catalyst for the oxygen electrode of an acid fuel cell.

Alkaline earth titanates, manganates, and cobaltates are soluble in hot, phosphoric acid. They are, therefore, unsuitable as catalysts for fuel cells of the type considered here.

Although some materials appear promising, the work reported here was too preliminary to decide definitely that oxide materials will or will not serve adequately as oxygen electrodes in a hot phosphoric acid fuel cell.

SECTION II

RECOMMENDATIONS

There are several fruitful areas of research in which appropriate work may well lead to a substitute for platinum and increased understanding of the electro-catalytic process involved. Of the materials studied here, barium ruthenate appeared to have promise as a model material, but much remains to be done to provide an understanding of its chemistry as an electrode.

The phase relations for the mixed oxides containing rare earths (*e.g.*, cesium and/or praeseodymium) and certain transition metals (*e.g.*, titanium, vanadium, niobium, and/or tantalum) should be elucidated in order to prepare suitable materials for testing. Then the acid stability tests should be made where still needed, and the electrochemical studies performed.

Appropriate electrodes of triphenylphosphine copper thiotungstate should be prepared and studied electrochemically.

SECTION III

INTRODUCTION

GENERAL

The fuel cell is related to the well-known "storage battery" through the fact that both convert chemical energy into electrical energy. The principal difference is pointed up by the words *fuel* and *storage*. The storage battery, a regenerative device, stores electrical energy by converting it to chemical energy for later release again as electricity. The fuel cell, on the other hand, can convert fuel into electrical energy continuously.

In ordinary use, fuel is burned and the heat thereby generated is used directly, or among other possibilities, it may be converted to steam which is used to power an electric generator. Other means to burn fuel and produce electric energy include magnetohydrodynamic generation. In a fuel cell, on the other hand, the chemical reaction between the fuel and oxidant produces, in the appropriate electrochemical device, electrical energy directly. For the simplest devices hydrogen and oxygen serve directly as fuel and oxidant. More complex systems are required in order to use fossil fuels or derivatives therefrom. Air is a practical and economical oxidant.

The fuel cell offers advantages of high efficiency at partial and at full load, silence, low-pollution, unattended operation, and construction in modular units to allow for optimum distribution of sites. There are, however, a number of areas where further research and development are needed to make fuel cells economically competitive so that they will make a significant impact on the energy conversion technology of the United States. A large factor in the economics of these devices is the cost of the catalyst used on the electrodes. Currently, platinum is the most widely used catalyst

in the acid fuel cell, the leading candidate for widespread use in electric power generation. For example, it is the catalyst for the United Aircraft device for power generation[1] which has had the most development, testing, and demonstration to date. The great cost of platinum affects the fuel cell economics by leading to high initial cost and to high replacement cost because platinum has a relatively short life-time. Another factor is that its catalytic action is not perfect and permits formation of intermediate peroxides cutting efficiency by about 40%. For these reasons a fruitful program of research would be to look for alternate catalysts which may not suffer from some of the disadvantages of platinum. An important auxiliary benefit could be to gain further understanding of the electrochemical processes involved and of the nature of pertinent catalytic materials.

The work reported here was based upon the assumption that the pertinent fuel cell for power generation would have hot phosphoric acid as an electrolyte. Again, this is used in the cell which is the forerunner[1]. Furthermore, attention was focussed upon the oxygen electrode, where the electrochemical efficiency loss appears to be greatest. Consequently, two required properties are stability in hot phosphoric acid and catalytic activity for the electroreduction of oxygen.

OBJECTIVES

The objectives of the project were to assess the potential of some selected transition metal oxides as electrocatalysts for fuel cells and to develop an understanding of the important material parameters for this application. It is a long-term goal, beyond the term of the contract, to establish an interrelationship between the structure, defect content, and concentration of dopants of metal oxides and their behavior as electrodes in low temperature fuel cells, with emphasis upon the cathode.

ORGANIZATION OF THE REPORT

In the remainder of the report, separate sections will be devoted to phase studies related to the discovery and preparation of new mixed oxide materials. Brief studies of the acid stability of some of these materials are reported. Electrochemical studies of those materials which appeared at the time to be potential catalysts for oxygen reduction at the cathode of a fuel cell are included.

Early in the course of the project the idea was conceived that the molecular structure of nitrogen-reducing enzymes might offer a clue to oxygen reduction catalysts. Consequently, some effort was aimed at producing pertinent compounds. A number of such compounds were made, and some of these are being subjected to tests involving solid electrodes. The concept and the chemistry involved in the preparation are sufficiently interesting to be reported here.

SECTION IV

ACID STABILITY

INTRODUCTION

A systematic program that integrated efforts in the acid stability and materials preparation (see Section V) studies was followed. Initially, acid stability testing was conducted using available and newly-synthesized oxide materials which showed potential for suitable electronic properties. These materials primarily were oxides containing first-row transition metals. This avenue of approach proved unsuccessful and emphasis, therefore, was shifted toward materials having potential for acid stability. Materials in this group were oxides containing tantalum or niobium. These oxides proved to be acid stable but are poor electronic conductors. Research, therefore, was focussed on new Ta- and Nb-containing oxides which could be modified chemically to enhance their electronic properties.

METHOD OF TEST

Stability in 85% phosphoric acid at a mininum of 100 °C was chosen as an initial screening test for candidate oxide materials. This test was conducted in two stages. A qualitative determination first was made by simply immersing powdered oxides in a bath of hot acid. Stability of a material was noted by observing apparent degradational processes (*i.e.*, dissolution/decomposition, solution color changes). Residues from these tests were examined by powder x-ray diffraction to determine any changes in phase constitution from the original, single phase, untreated material. A material which did not show apparent degradation during this stage was fashioned into a rod- or disc-shaped body and sintered at an appropriate temperature. This body was placed in a Pt-wire basket which then was immersed and rotated in a bath of hot acid. Possible degradation of the material was monitored gravimetrically. In most

cases this test was performed first at 110 °C and then at 150 °C for durations of up to one month.

RESULTS

The initial stage of this investigation concentrated on the acid stability characteristics of oxides containing first-row transition metals previously prepared in this laboratory. For this stage, however, only those materials were chosen which, from stoichiometric considerations, had at least the potential to be metallic or semiconducting. Materials from the following systems were tested:

a. $SrMnO_{3-x}$, $0 \leq x \leq 0.35$ (see ref. 2 for complete details of the system)

b. $BaMnO_{3-x}$, $0 \leq x \leq 0.28$ (see ref. 3 for complete details)

c. $Ba_{1-y}Sr_yMnO_{3-x}$, (see ref. 4 for complete details)

d. $BaCoO_{3-x}$ and $BaNiO_{3-x}$ (see ref. 5 and 6 for complete details)

e. $SrMnO_{3-x}$ - "manganese oxide" (see ref. 7 for complete details)

These systems feature materials having numerous crystal structures related to and including the perovskite type. Moreover, the transition metal (Mn, Ni, or Co) can exist in multiple oxidation states, a phenomenon (nonstoichiometry) recently shown to be important in some types of catalytic activity (*i.e.*, CO oxidation and NO_x reduction). None of the materials in these systems withstood attack by hot phosphoric acid. It was noted, however, that the low temperature form of $SrMnO_{3-x}$ ($0 \leq x \leq 0.10$), with a so-called four-layer hexagonal structure[2] was not attacked at room temperature. The compound began to dissolve at 60 °C. It was thought that this material might be rendered more acid stable by suitable partial substitution (solid solution) of acid stable, oxide end-members having similar, perovskite-related structures. $BaTiO_3$ and $SrTiO_3$ were chosen as candidate materials for this purpose in view of their resistance to some acids. However, this effort was curtailed when tests showed that even these materials undergo dissolution in hot phosphoric acid.

Another series of nonstoichiometric transition metal oxide materials of the perovskite type, $La_{(2/3)+x}Ti^{3+}_{3x}Ti^{4+}_{1-3x}O_3$ ($x \leq 1/3$) appeared promising. This series contains solid solutions with properties ranging from metallic ($LaTi^{3+}O_3$) through semiconducting to insulator ($La_{2/3}Ti^{4+}O_3$). It had been suggested[8] that these materials were stable in cold HCl, HNO_3, perchloric acid and in hot, dilute HNO_3, and in boiling perchloric acid. They were slowly attached by aqua regia. Phases in this series, as well as Gd and Sm analogues, were prepared either in this laboratory or obtained from an external source (Mr. Neil Loeffler, University of Tennessee Space Institute). Similar materials, $La_{0.75}A_{0.25}Ti^{3+}_{0.75}Ti^{4+}_{0.25}O_3$ (A = Sr or Ca) were also prepared in cooperation with Mr. Loeffler. All materials were tested and found to dissolve in hot phosphoric acid and 3N sulfuric acid.

In the second stage of this study, oxide materials containing Ru, Ta, and Nb were investigated. $BaRuO_3$, $SrRuO_3$, and $CaRuO_3$, characterized as having "good" conductivity[9,10] and metallic conductivity[11] were tested. Only $BaRuO_3$ was found to be stable (110 °C, 5 days) in phosphoric acid. All of the niobium- and tantalum-containing phases that were prepared (see Section V) showed remarkable resistance to attack by hot phosphoric acid. Many of these phases, however, are poor conductors and it would be necessary to enhance their electronic properties, perhaps, by suitable doping.

SECTION V

PHASE STUDIES AND MATERIALS PREPARATION

Perovskite materials in the series $La_{(2/3)+x}Ti^{3+}_{3x}Ti^{4+}_{1-3x}O_3$ ($x \leq 1/3$) and in the series $La_{0.75}A_{0.25}Ti^{3+}_{0.75}Ti^{4+}_{0.25}O_3$ (A = Sr or Ca) were synthesized. The latter materials were chosen hoping to enhance the acid stability of the first series without a sacrifice in electronic conductivity. Materials were prepared from La_2O_3 [from $La(OH)_3$], TiO_2, Ti metal, and $SrTiO_3$ or $CaTiO_3$ starting materials, proportioned to yield the desired stoichiometries. The starting materials were mixed then melted and cooled in high purity Mo crucibles in an induction furnace containing a "gettered" argon atmosphere. The resulting products, examined by powder x-ray diffraction, were found to be single-phase perovskites (non-cubic). These materials were utilized subsequently for electrochemical and acid stability experiments.

$BaRuO_3$, $SrRuO_3$, and $CaRuO_3$ were prepared from the appropriate alkaline-earth carbonate and RuO_2 or Ru metal. The blended starting materials were reacted in gold envelopes at 1000 °C in air for one day. $SrRuO_3$ and $CaRuO_3$ have the perovskite structure while $BaRuO_3$ has a so-called nine-layer rhombohedral-hexagonal structure in which face-sharing of Ru-containing oxygen octahedra occurs[9]. As indicated in Section IV only $BaRuO_3$ remains stable in phosphoric acid and was used in subsequent electrochemical experiments. The acid stability of $BaRuO_3$ was somewhat unexpected as the phase $Ba_{0.9}Sr_{0.1}MnO_3$ (< 1265 °C in air) has the same crystal structure[4] yet is attacked by phosphoric acid. Phase transitions in or reduction of $BaRuO_3$ were not detected up to 1600 °C in air by differential thermal and thermogravimetric analysis. Significant vaporization, presumably of Ru through oxidation to gaseous RuO_2 or RuO_3, was observed above 1500 °C. This vaporization precludes the preparation of dense sintered discs at these elevated temperatures. For example, a pressed disc of

initially single phase $BaRuO_3$ was fired 22 hours at 1500 °C. The product consisted of two phases, $BaRuO_3$ plus a ruthenium-containing phase richer in barium. If dense discs are necessary for electrochemical testing, $BaRuO_3$ could be hot-pressed or isostatically pressed at lower temperatures (< 1500 °C) to prevent loss of compositional integrity.

Past experience in this laboratory has shown that oxide materials containing Nb_2O_5 or Ta_2O_5 resist attack by many acids. For this reason, several of these oxides were synthesized and tested with phosphoric acid prior to initiating an investigation of new materials. In the system Ta_2O_5-TiO_2, Roth and Waring[12] at NBS showed that TiO_2 (rutile) can accommodate as much as 10 mole percent Ta_2O_5, depending on temperature, without gross structural changes. A composition midway in this range, $Ta_2O_5 \cdot 19TiO_2$, was chosen and prepared using high purity TiO_2 and Ta_2O_5 starting materials. After a preliminary calcination at 1000 °C for three days, this mixture was fired at 1600 °C for one day and quenched in water. The final blue-black product consisted of single-phase rutile solid solution as revealed by powder x-ray diffraction analysis. This material was utilized for acid and electrochemical testing. The compounds $V_2O_5 \cdot 9Nb_2O_5$ and $V_2O_5 \cdot 9Ta_2O_5$ were also prepared according to methods in reference 13 and tested in hot phosphoric acid.

In view of the apparent resistance of Ta_2O_5- and Nb_2O_5-containing oxides to attack by hot H_3PO_4, an investigation of new materials based on these oxides was initiated. Cerium oxide was chosen as an additional component because the cerium cation can exist in crystalline phases in mixed 3+, 4+ oxidation states. This could enhance the probability for reasonable electronic conductivity of potential electrode materials. Furthermore, cerium oxide was shown to be a catalyst for related gas phase reactions[14]. When CeO_2 reacts with Ta_2O_5 (or Nb_2O_5) at elevated temperatures, compounds are formed that contain the reduced oxidation state, Ce^{3+}, even

under oxidizing conditions as in air. In the Ta_2O_5-cerium oxide system, three compounds, $CeTa_7O_{19}$, $CeTa_3O_9$, and $CeTaO_4$ are stable. The crystallographic and magnetic properties of these, as well as additional, unusual phases, were detailed fully in this laboratory. The phases $CeTa_3O_9$ and $CeTaO_4$ resist attack by hot H_3PO_4, but, apparently, are not good conductors. Attempts, therefore, were made to enhance the electrical conductivity by altering the Ce^{3+} content toward mixed Ce^{3+}/Ce^{4+} variants for each phase.

$CeTa_3O_9$ can be reformulated as $Ce_{1/3}TaO_3$. Single crystal and powder x-ray diffraction studies revealed that this material has the perovskite structure which is distorted to orthorhombic symmetry. The formulation, $Ce_{1/3}TaO_3$, indicates that the A-sites of this perovskite (ideally ABO_3, A/B = 1.0) are not fully occupied, $A_{Ce}/B_{Ta} = 1/3$. Attempts, therefore, were made to establish Ce^{4+} cations at the A-sites by appropriate substitutions of A^{2+} cations. This would lead to mixed Ce^{3+}/Ce^{4+} oxidation states and possibly to enhanced conductivity. The substitution mechanism can be formulated as,

$$[Ce^{3+}_{(1/3)-x}Ce^{4+}_{x/2}A^{2+}_{x/2}]TaO_3,\ x < 1/3 \qquad (1)$$

The feasibility of this type of substitution was tested by additions of Sr^{2+} according to,

$$[Ce^{3+}_{7/30}Ce^{4+}_{1/20}Sr_{1/20}]TaO_2,\ x = 1/10 \text{ in (1)} \qquad (2)$$

Single phase perovskite products could not be synthesized and this effort was discontinued. It is noted, however, that $Ce_{1/3}TaO_3$, an acid stable material, might be used as a component to enhance the acid stability of perovskite and perovskite-like phases of the first-row transition metal oxides previously tested (see Section IV).

Attempts to vary the Ce^{3+}/Ce^{4+} content of $CeTaO_4$ met with success. Phase equilibrium studies (reaction and quenching of materials from elevated temperatures), single crystal and powder x-ray diffraction analysis, thermogravimetric analysis,

and magnetic susceptibility measurements were utilized to completely define phase relations and oxidation-reduction reactions in the system $CeTaO_4$-oxygen (in air). $CeTaO_4$ is stable in air from 1265 °C to a melting point near 1960 °C. At 1265 °C, the material oxidizes (reversibly) according to,

$$3CeTaO_4 + 1/2\ O_2 \xleftrightarrow{1265\ °C} CeTa_3O_9 + 2CeO_2 \qquad (3)$$

Notice that the bulk composition of the decomposition products is expressed by $Ce_3Ta_3O_{13}$ or $CeTaO_{4.33}$. The reaction proceeds to the right rapidly within the range 1265°-1100 °C but sluggishly between 1100°-1000 °C. If $CeTaO_4$ is quenched to room temperature and reheated below 1000 °C, or, if the material is rapidly cooled from above 1265 °C to below 1000 °C, the oxidation-decomposition reaction (3) is completely by-passed. Instead, $CeTaO_4$ absorbs oxygen (oxidizes) according to,

$$CeTaO_4 + 1/2\ x\ O_2 \longrightarrow CeTaO_{4+x} \qquad (4)$$

The x parameter in $CeTaO_{4+x}$ is variable but temperature dependent. Four distinct reaction series were defined for the system $CeTaO_4$-oxygen ($CeTaO_{4+x}$). A summary of the observed reactions and reaction paths is given in the flow diagram provided. The following symbols are used:

(←——→), rapid, reversible reaction

(←- - - -→), sluggish, time dependent, but reversible reaction

(- - - - - - →), sluggish, non-reversible reaction

(←- - - —→), reversible reaction but rapid or sluggish in the direction indicated.

It is emphasized that every phase shown in the flow diagram can be prepared by the pertinent reaction path and can be quenched (and retained) to room temperature. Within series 2, 3, and 4, x varies continuously with temperature. For this reason, only typical x parameters in $CeTaO_{4+x}$ are given for selected temperatures. Ce^{3+}/Ce^{4+} contents can be computed for given x parameters using $Ce^{3+}_{1-2x}Ce^{4+}_{2x}TaO_{4+x}$. This formulation was confirmed by magnetic

The System $CeTaO_{4+x}$ ($0 \leq x \leq 0.5$) in Air

$CeTaO_4 \xleftrightarrow{1265°} CeTa_3O_9 + CeO_2$ (decomposition products) Series 1

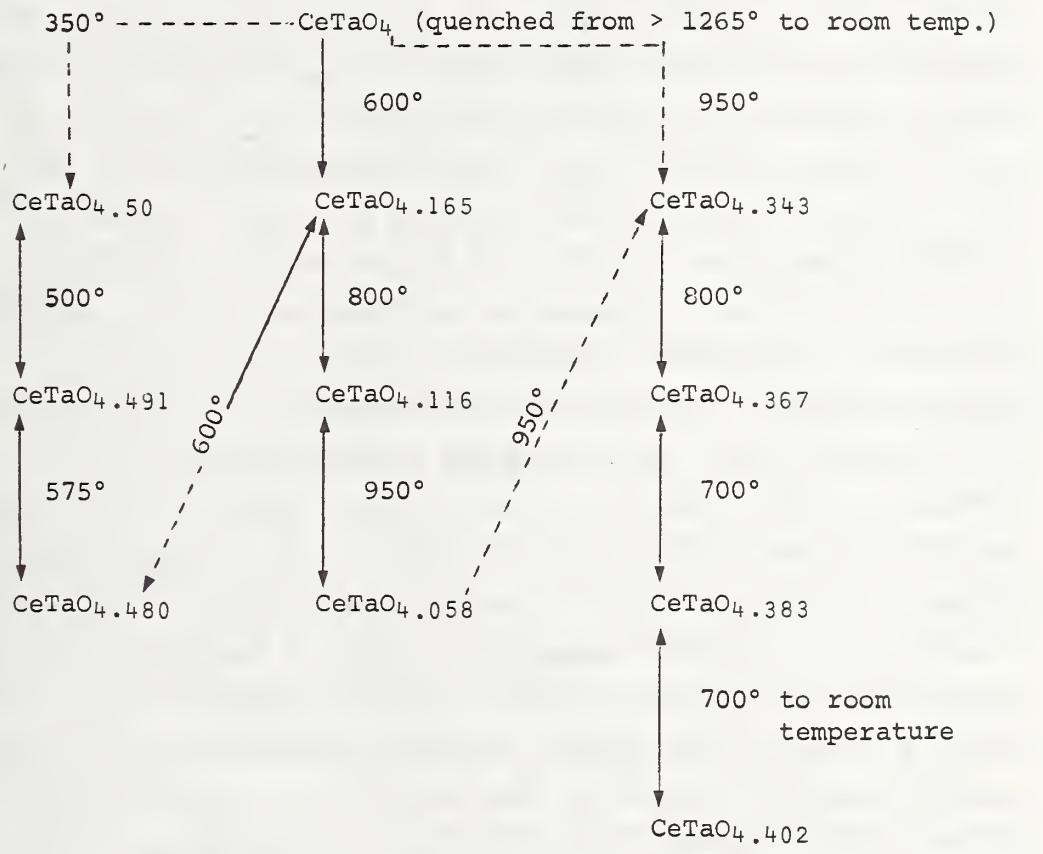

Series 2 Series 3 Series 4

susceptibility measurements.

Starting with preformed $CeTaO_4$ (> 1265 °C, quenched to room temperature) any reaction series can be initiated by heating the materials within the pertinent temperature range indicated. Once series 4 phases (not related crystallographically to $CeTaO_4$) are formed, however, series 3 and 2 materials subsequently will not form. Series 4 materials will transform to series 1 phases at elevated temperatures. Within each series, oxidation-reduction reactions are almost instantaneous and reversible, with x being a function of temperature. Reactions between any two series are generally sluggish and not necessarily reversible. For example, reactions in series 3 can be followed (thermogravimetrically) continuously to at least 950 °C (x = 0.058). Phases in this series are crystallographically related to $CeTaO_4$. If the sequence is stopped within the 900-950 °C interval, and the series 3 material is maintained at constant temperature, series 4 materials will slowly develop over several hours. Thus the transition from series 3 to series 4 materials, although indicated at 950 °C, can proceed sluggishly between at least 900-950 °C. Another example is the oxidation reaction which results in the formation of completely oxidized cerium phase $CeTaO_{4.50}$ (350 °C) from $CeTaO_4$ or from any series 3 phase. This reaction proceeds over periods of at least several days. Indeed, one sample of $CeTaO_4$ was maintained at 350° for 61 days to insure formation of a completely oxidized material which could be used for further experimentation. Phases in series 2, 3, and 4 will transform to series 1 phases when reacted above 1000 °C. Once $CeTaO_4$ is decomposed (series 1, < 1265 °C), further reactions at lower temperatures, of course, are precluded.

The complex reactions observed for the $CeTaO_{4+x}$ system provided the impetus to investigate similar Ta- and Nb-containing materials. The phases $Pr^{3+}TaO_4$ and $Ce^{3+}NbO_4$ were reported by Bodiot[15]. $PrTaO_4$ was found to have an x-ray diffraction powder pattern (unindexed) similar to that of $CeTaO_4$. $CeNbO_4$, however, has the monoclinic (M)-fergusonite structure (see, for example, ref. 16) at room

temperature. These materials were also prepared attempting to vary their Ln^{4+}/Ln^{3+} contents by appropriate annealing at low temperatures. $PrTaO_4$ is isostructural with $CeTaO_4$, and the magnetic and crystallographic properties of the material have been characterized. In air, $PrTaO_4$ does not undergo the reaction series shown by $CeTaO_4$. This can be attributed to the difficulty of oxidizing Pr^{3+} to Pr^{4+}. Indeed, Pr_6O_{11} (= $PrO_{1.833}$) is the highest oxide that is stable in an air environment. $PrTaO_{4+x}$ might be prepared at much higher oxygen pressures. As $PrTaO_4$ is isostructural with $CeTaO_4$ and because it does not oxidize, it is conceivable that this component can be utilized to stabilize $CeTaO_{4+x}$ phases at specific x values and at lower temperatures. For example, series 3 $CeTaO_{4+x}$ phases are stable only between 600 °C to about 900 °C, but may be quenched to room temperature. If these materials are subjected to high oxygen activities at lower temperatures, complete oxidation to $CeTaO_{4.50}$ ultimately results. Suppose $PrTaO_4$ is introduced in solid solution with $CeTaO_4$, to give, for example, the composition $(Ce^{3+}_{0.5}Pr^{3+}_{0.5})TaO_4$. If it were possible to completely oxidize this phase the maximum oxygen content would be $(Ce^{4+}_{0.5}Pr^{3+}_{0.5})TaO_{4.25}$, x = 0.25, but not $(Ce^{4+}_{0.5}Pr^{4+}_{0.5})TaO_{4.5}$. The stoichiometry, when x = 0.25, however, is never encompassed by the x parameter variation within any given $CeTaO_{4+x}$ series. If phases with x > 0.25 cannot be obtained, then x parameters typical only of series 3 phases remain possible. Single-phase $(Ce^{3+}_{0.5}Pr^{3+}_{0.5})TaO_4$ was prepared and annealed at temperatures < 900 °C in air. Only series 3 type phases were obtained.

The Ce^{4+}/Ce^{3+} content in $CeNbO_4$ (not isostructural with $CeTaO_4$) also can be varied according to preliminary data. Furthermore, x-ray diffraction data suggest that more than one reaction series is operative. One series appears to be characterized by oxidation together with exsolution of CeO_2 from $CeNbO_4$. Such a process would yield materials having variable Ce^{4+}/Ce^{3+} contents and vacancies on the Ce sublattice.

SECTION VI

ELECTROCHEMICAL MEASUREMENTS

INTRODUCTION

Potential materials for the oxygen electrode in fuel cells must be screened, under conditions similar to those encountered in a real cell, for both stability and catalytic activity. Although, ultimately, any electrode found must be tested by construction of an actual cell, there are simpler methods of screening available that can be used to select the most likely candidates. Such techniques were initiated during the course of this study.

Two basic approaches to the electrochemical characterization of oxide electrodes were utilized. The primary method was to subject the samples to a potentiodynamic scan ranging from the hydrogen evolution potential to anodic potentials greater than the expected potential for oxygen evolution. This was performed with the sample in electrolytes similar to those used in real fuel cells. If a cathodic current were to be observed in the potential range of oxygen reduction, the possibility that the current was due to chemical instability would have to be checked before it could be ruled out. A secondary, galvanostatic, method was to observe the potential at various fixed currents on both the anodic and cathodic side of the equilibrium potential for several oxidation-reduction couples dissolved in varying electrolytes.

EXPERIMENTAL ARRANGEMENTS

Description of Experimental Set-up

As shown in Figure 1, the experimental arrangement is straightforward. Minor details such as a compensator for the recorder and switching circuits for AC work have been omitted. A detailed discussion of the cell and of the electrode format used will follow later in this section.

The potentiostat is a commercial unit capable of providing slightly more than 100 ma. Its control voltage is provided by the output of the control voltage amplifier which is driven by the

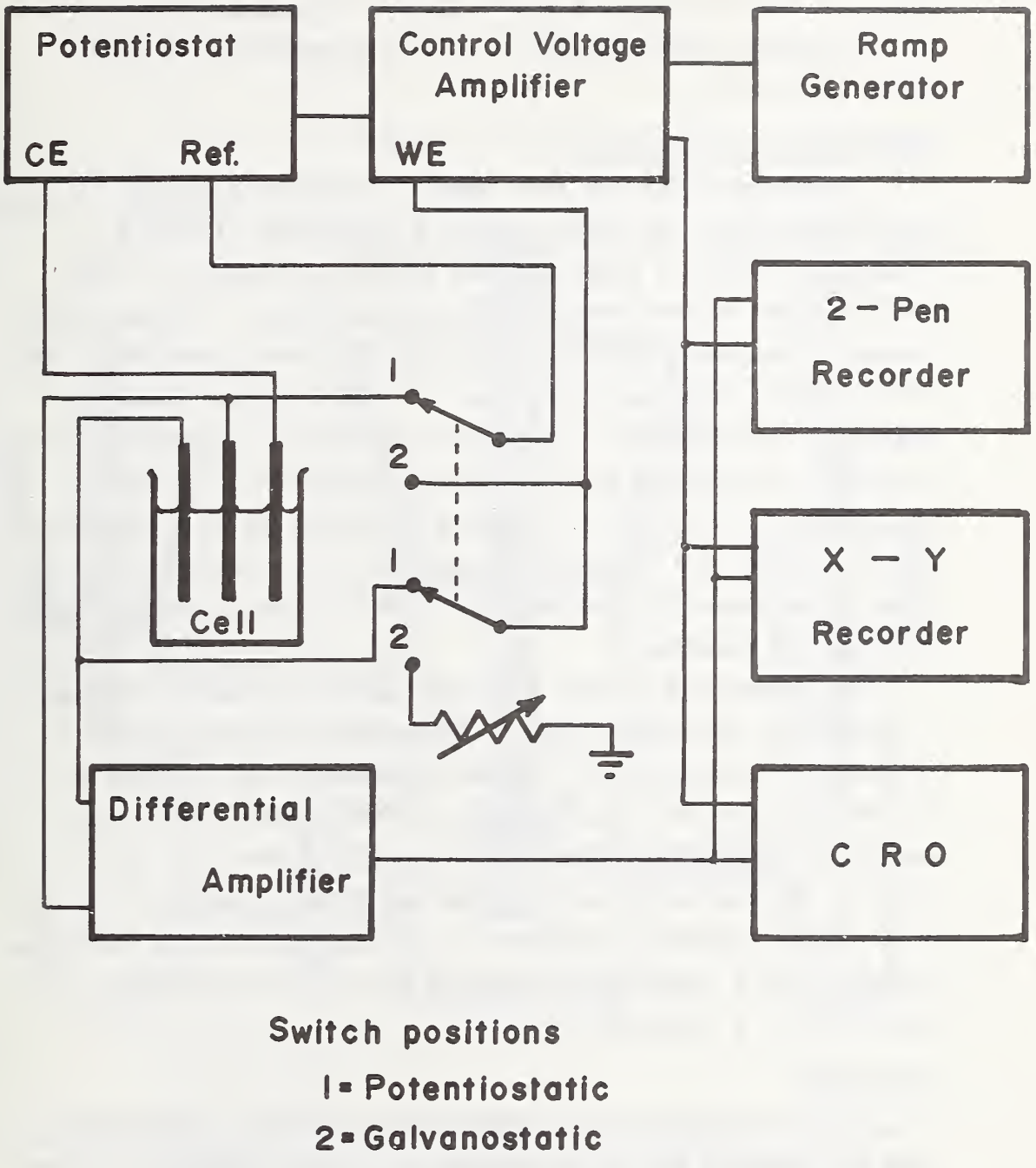

Figure 1. Block diagram of electrochemical instrumentation.

ramp generator. The ramp generator consists of a motorized multi-turn potentiometer wired as a voltage divider. Ramp rates range from 1.6×10^{-3} V/sec to 8×10^{-2} V/sec. Adjustment of the gain of the control voltage amplifier gives the capability of rates up to 1.6 V/sec.

Description of Cells Used

Depending on the choice of sample electrode, two types of cells were used. The first, used with electrodes of Type I (described later) is shown in cross section in Figure 2. This cell consists of four interconnected compartments. The sample-to-counter electrode connection is through a fritted glass disc. The two remaining compartments are for a Pt and a calomel reference electrode, respectively. Provisions were made in the sample container for stirring and for bubbling gasses over the sample. The sample is electrically connected to the system by a threaded stainless steel rod which is protected from the electrolyte by glass tubing sealed to the sample by a Teflon gasket, in the manner of Stern and Makrides[17].

The second type of cell which was used, is intended for Type II electrodes (described later). Essentially, it was a beaker contained in a water bath. The entire assembly was enclosed in an insulated box with feed-throughs for electrical contact and gas input. The counter electrode was platinum black and of Type II, and the reference electrode was either a smooth Pt strip or a calomel electrode. For most of the experiments, the reference was placed in a compartment connected to the electrolyte near the sample by a capillary.

Electrodes

For convenience, in this report the two kinds of electrodes used are labelled as Type I and Type II. Type I electrodes (shown in cross section as part of Fig. 2) were made from poly- or mono-

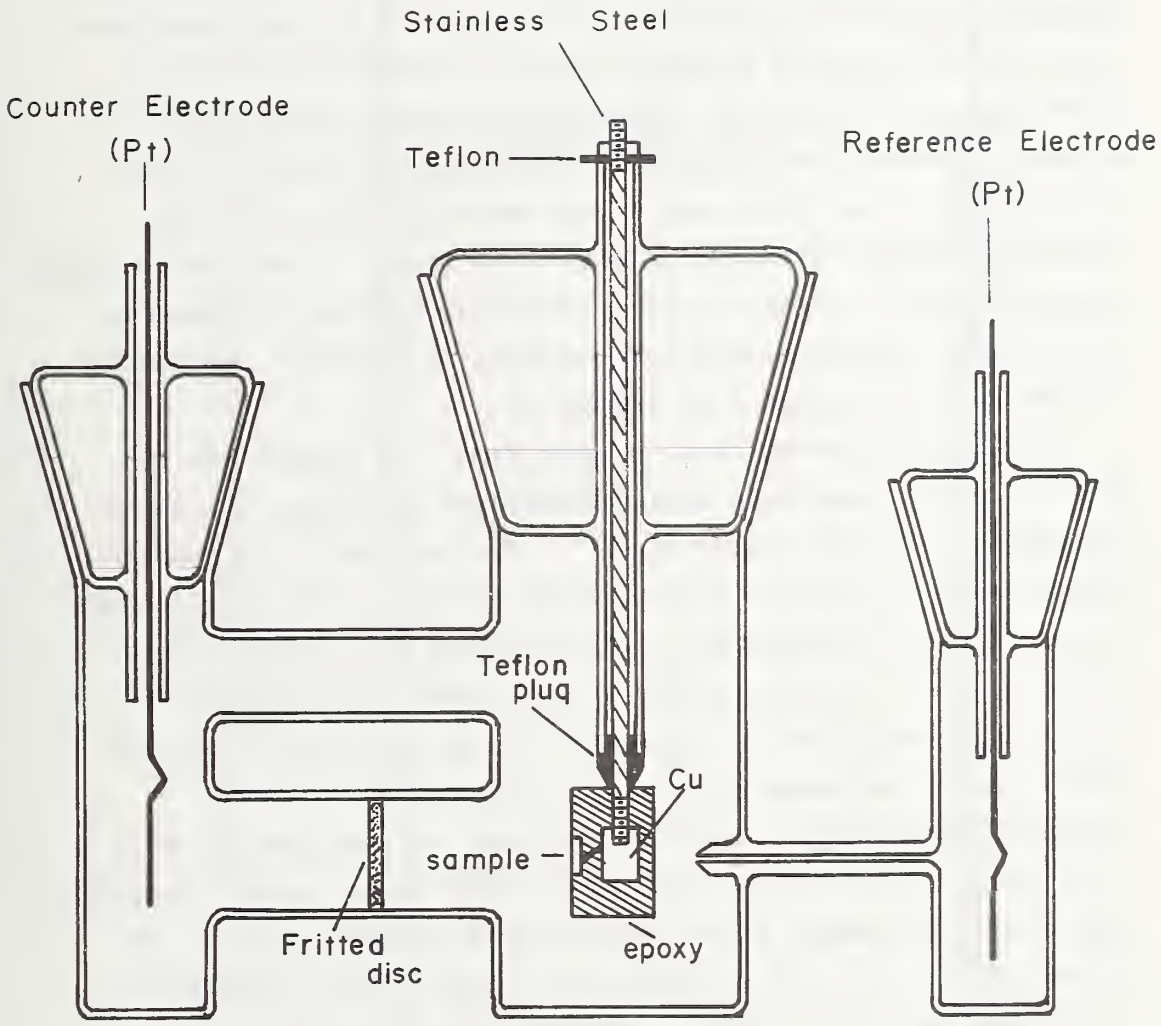

Figure 2. Electrochemical cell used at room temperature with Type I electrodes. This is a cross section of three of the four compartments. Compartment 4, which contains the Calomel reference, is situated behind the compartment for the Pt reference. A type I electrode is also shown in cross section. The heavy black line, connecting sample and Cu block, denotes a Pt wire for electrical contact.

crystalline samples or from sintered powders. A Pt wire lead was attached to the rear surface of the sample by appropriate means (indium soldering, peening, silver paste, etc.), and the other end of the lead was soldered to a Cu block about 1 cm on each edge. This assembly was placed in a mold made from Al foil and cold-setting epoxy mounting compound was poured in. The mold was then placed in an evacuated chamber in order to remove air from any pores and allow them to be filled by the epoxy. After a few minutes, the mold was returned to atmosphere and allowed to set for 24 hours. When set, the Al foil was stripped off and the mounted sample was ground to a convenient shape. A hole was drilled through one end into the Cu block, and this was then threaded to receive the stainless steel rod previously mentioned. The sample surface was then ground with 600 grit.

Type II electrodes (Fig. 3) were made from powders and are porous. These electrodes were manufactured by a modification of the method of Neidrach and Alford[18]. The substrates for Type II electrodes were strips 1.5 cm by 15 cm of either electrodeposited Ni or stainless steel screen, 0.017 cm thick with approximately 20% open area. This was coated with a 0.005 cm thick layer of Teflon film except for two regions. At one end, about 5 cm were left uncoated for purposes of electrical connection to the measuring instruments. Close to the other end, an area of about 0.5 cm by 1.5 cm was left clear on one side of the strip. A paste composed of the sample powder mixed with #30 Teflon emulsion was placed on this area and covered with Al foil. The electrode was hot pressed at 320 °C under an applied load of 2×10^3 kg for 2 minutes. When cool, the Al foil was removed by immersion in 6 mol/l NaOH.

Table 1 shows the electrochemical systems that were examined.

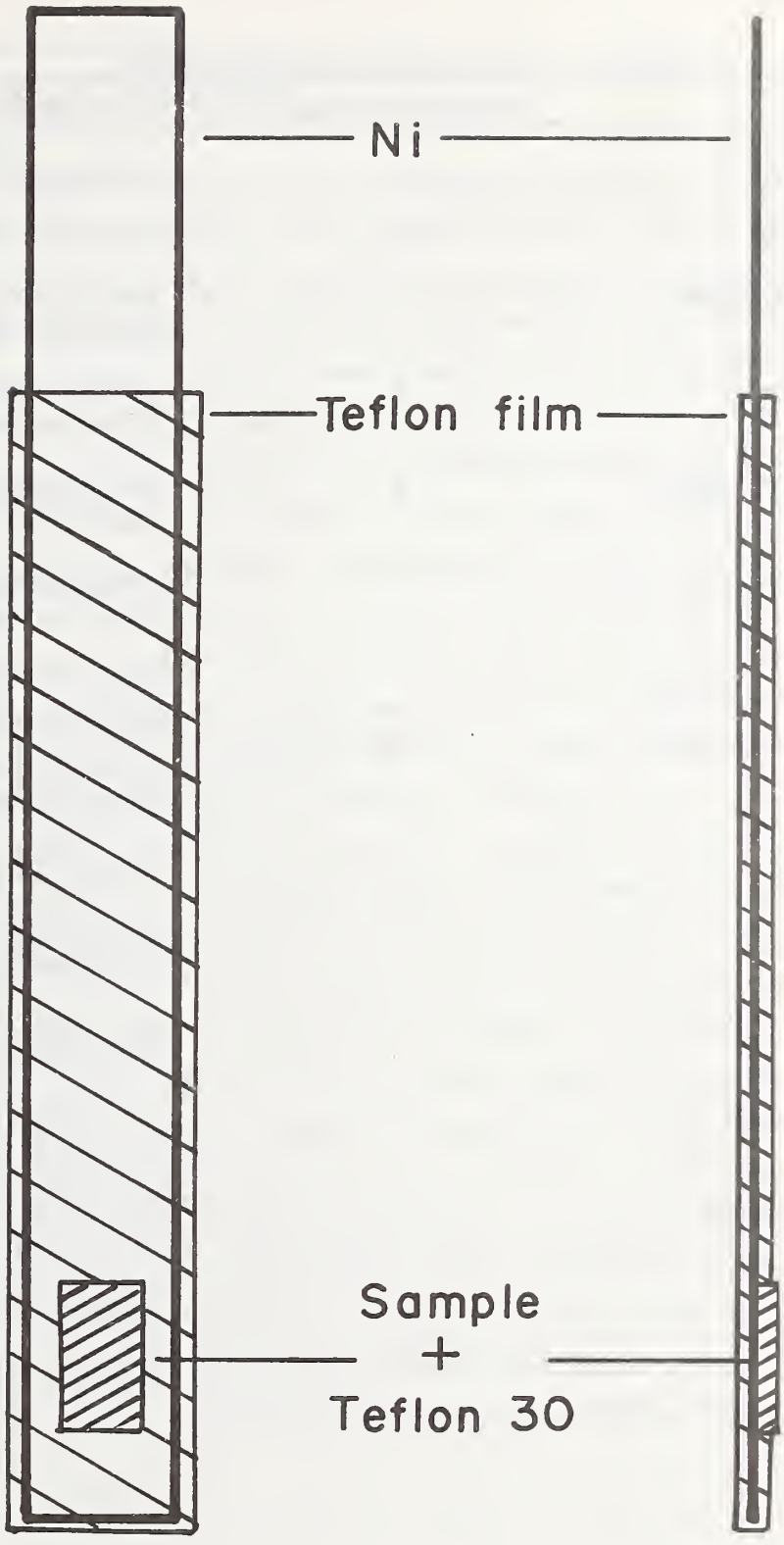

Figure 3. Type II electrode shown in front view and cross section.

Table 1. ELECTROCHEMICAL EXPERIMENTS

Material	Electrode Type	Study Method
TiO_2:5% Ta	I	potentiodynamic
TiO_2:5% Ta	II	potentiodynamic
TiO_2:H_2 reduced	I	potentiodynamic galvanostatic
TiO_2:0.1% Nb	I	potentiodynamic galvanostatic
$La_{0.92}TiO_3$ (nom.)	I	potentiodynamic galvanostatic
$La_{0.75}TiO_3$ (nom.)	I	potentiodynamic galvanostatic
$La_{0.75}Ca_{0.25}TiO_3$	I	potentiodynamic
$La_{0.75}Sr_{0.25}TiO_3$	I	potentiodynamic
$Na_{0.7}WO_3$	I	potentiodynamic galvanostatic
$BaRuO_3$	I	potentiodynamic
$BaRuO_3$	II	potentiodynamic galvanostatic
$SrTiO_3$:0.03% Nb	I	potentiodynamic galvanostatic
$SrTiO_3$:0.15% Nb	I	potentiodynamic galvanostatic
TiO_2 as grown	I	potentiodynamic galvanostatic
Ni	II	potentiodynamic
Pt black	II	potentiodynamic

Potentiodynamic Measurements

Titanates -

Voltammetric scans of the titanates were done in both 5M and concentrated phosphoric acid electrolytes with voltage scan range of the order of 10 volts. Normal procedure was to sweep the potential at a linear rate from values more negative than required for hydrogen evolution to those more positive than needed for oxygen evolution. This was done at room temperature and at 60 °C nominal.

On the basis of behavior, the samples studied may be separated into three groups. The first of these, ($SrTiO_3$:0.03% Nb and $SrTiO_3$:0.15% Nb) is soluble in phosphoric acid and will not be discussed in this section. The second group (TiO_2 as grown, TiO_2: 5% Ta, TiO_2:0.1% Nb, TiO_2:H_2 reduced) gave I-V curves typified by Figure 4. Starting at a potential yielding good evolution of H_2 and scanning in an anodic direction, a peak due to oxidation of H_2 was first observed followed by a region of zero current. At about 2.5 volts positive vs. S.C.E., a sizeable current began to flow. On the reversed sweep direction there was no observable negative current until the potential for H_2 evolution was reached. Bubbling of oxygen gas over the electrode yielded no detectable response.

The third group of samples ($La_{0.75}TiO_3$, $La_{0.92}TiO_3$, $La_{0.75}Sr_{0.25}TiO_3$, and $La_{0.75}Ca_{0.25}TiO_3$ - all values nominal) gave a family of I-V curves (Figure 5) that appear to depend on the value of x in the generalized formula La_xTiO_3. (Addition of Sr^{+2} or Ca^{+2} yields an effective new x value.) Starting with $La_{0.75}TiO_3$ fairly large anodic currents were drawn at potentials on the order of +2 volts. As indicated in Fig. 5, however, these currents fell off with continued cycling of the potentiodynamic sweep. As x was increased, there was a shift toward higher anodic potentials for

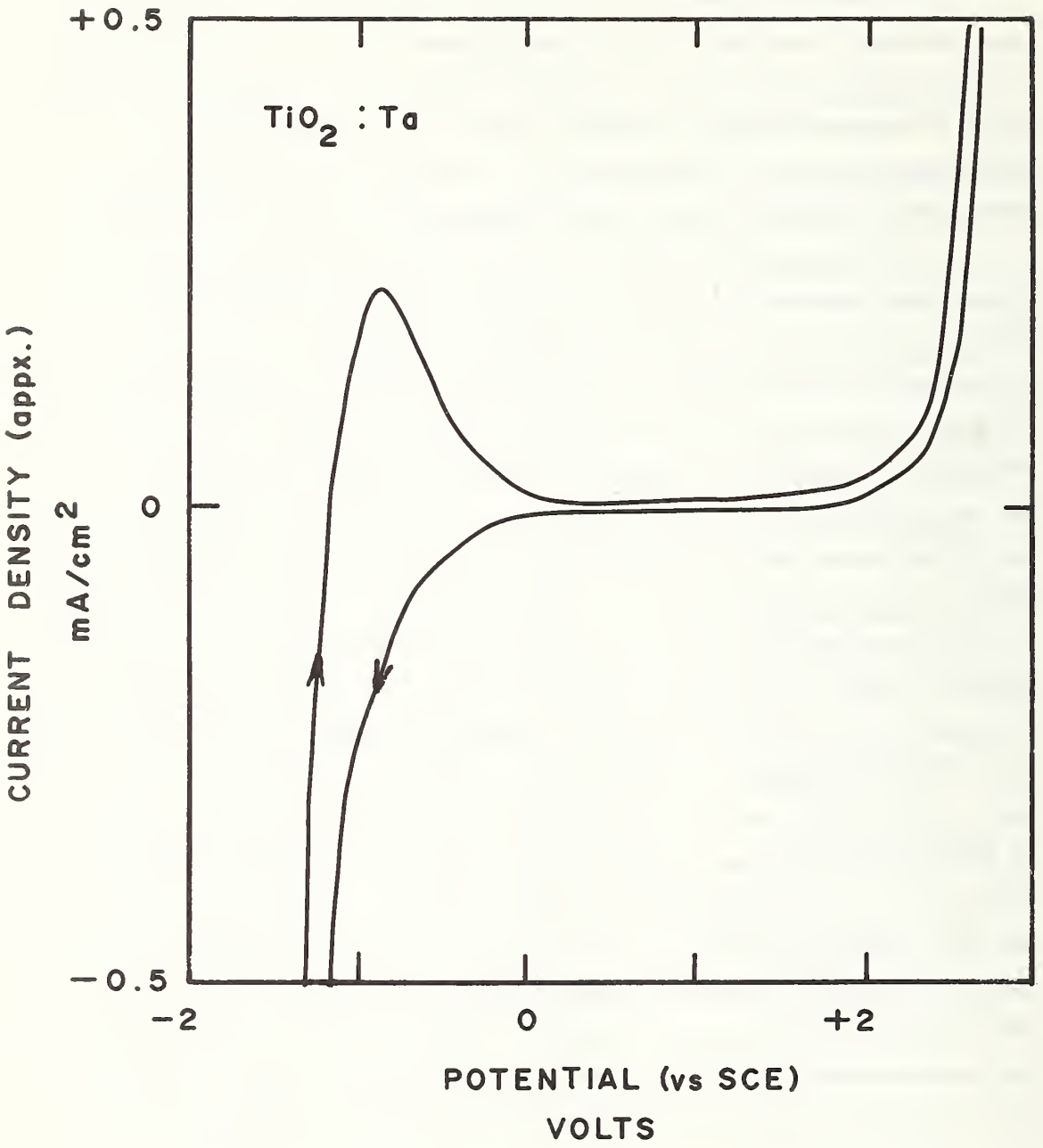

Figure 4. Current-potential curve for 95 TiO_2: 5 Ta_2O_5 in 5 mol/l H_3PO_4 at room temperature. Type I electrode configuration.

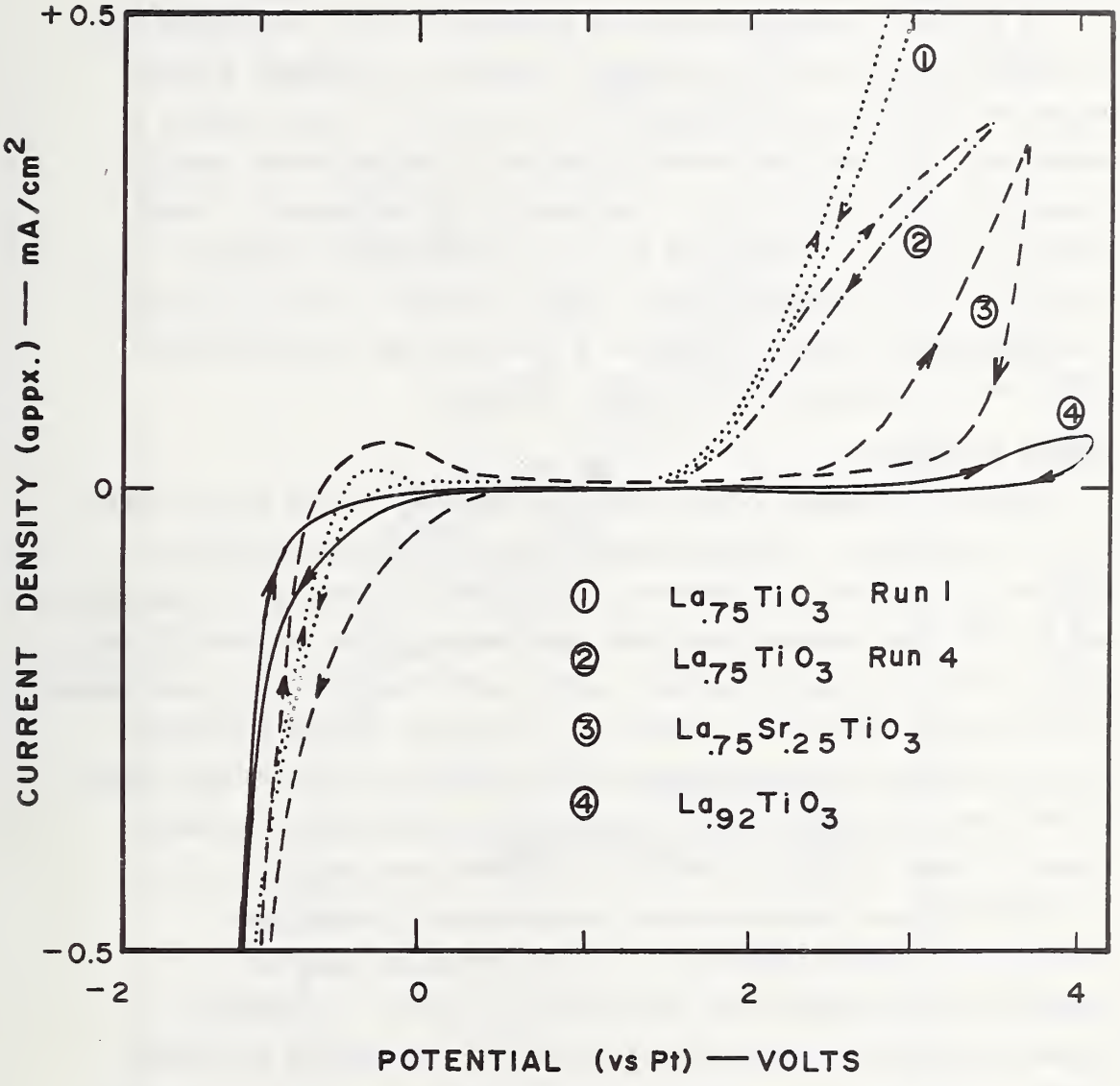

Figure 5. Current-potential curves for the Lanthanum Titanates at room temperature. Type I electrodes in 5 mol/l H_3PO_4.

current flow, until x = 0.92 where the observed current approached zero. There was no visible evolution of oxygen, and bubbling of oxygen over the electrode gave no response.

Tungsten Bronze -

A $Na_{0.7}WO_3$ single crystal was subjected to the same conditions as above. Starting at the hydrogen evolution potential, a large negative current was observed. As the scan went toward anodic potentials the positive current peak due to oxidation of hydrogen appeared (much larger than in the case of the titanates). The current then fell to zero and as the potential went positive, the surface of the electrode changed color and after a short positive transient the current returned to a low value and remained low. There was no indication of response to oxygen.

Barium Ruthenate -

Barium ruthenate, $BaRuO_3$, was the subject for the major portion of the experiments. Potentiodynamic scans were performed with samples in a number of different electrolytes at both room temperature and 60 °C. The electrolytes used were concentrated phosphoric acid, 6 mol/l NaOH, 1:1 H_3BO_3-$Na_2B_4O_7$, and 4 mol/l NaOH with H_2O_2 additions.

Although there was a great deal of scatter in the magnitudes of the currents observed at particular potentials, the overall shape of the curve for each $BaRuO_3$ electrode was essentially the same. Figure 6 shows a typical result for concentrated phosphoric acid at 60 °C. Visual observation of the electrode showed both hydrogen and oxygen evolution. Oxygen evolution began at potentials less anodic than the peak at + 0.9 V. In addition, visual observation indicated dissolution of the $BaRuO_3$ as current flowed. This is also evident in the I-V curves, since the observed currents decrease linearly with number of scans (ranging from hydrogen evolution to oxygen evolution). The scatter in the current for a fixed potential scan was about one order of magnitude when all electrodes were compared.

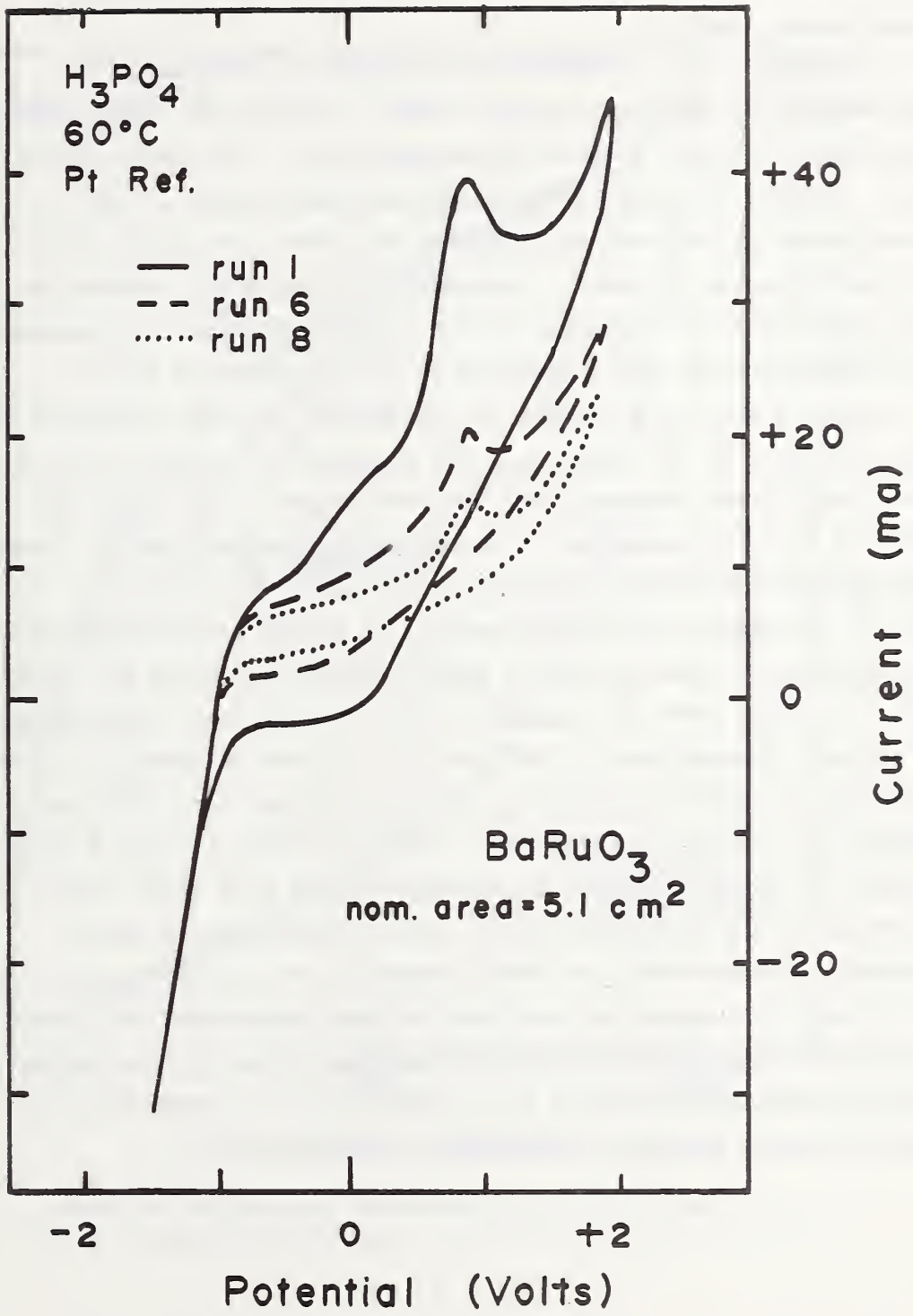

Figure 6. Current-potential curves for a Type II $BaRuO_3$ electrode in concentrated phosphoric acid at 60 °C. The decrease in current with time is probably related to dissolution of the sample.

Observed responses to oxygen bubbling vary with individual electrodes. Some electrodes exhibit a change (Figure 7) while others appear inert.

Voltammetry in 1:1 saturated H_3BO_3:$Na_2B_4O_7$ electrolyte at room temperature differs from both acidic and alkaline (discussed later) media. Figure 8 shows the results over a limited sweep range. A wider potential sweep shows that the results of the limited sweep illustrated are extended to greater potentials with only small changes in shape. Interestingly, the sharp changes in slope associated with hydrogen and/or oxygen evolution, are missing. Also missing are the peaks observed in acid or alkaline media.

Figure 9 shows the results of voltammetry for two electrodes in 6 mol/l NaOH at 60 °C. Note that the presence of O_2 gives rise to fairly significant changes. The observed shape of the curves is different from that observed in concentrated phosphoric acid. Other electrodes yielded similar responses although in one case the reaction to oxygen addition was small. It should be noted that the overall shape of these curves is similar to that observed for RuO_2 on Ti in 4 mol/l NaOH, by O'Grady, *et al*[19]. Because of this similarity, the effects of additions of 0.007 mol/l H_2O_2 were studied for a 4 mol/l NaOH electrolyte on $BaRuO_3$ electrodes. Figure 10 shows the effect as compared to a smooth Pt electrode. Note that there is only a small increase in cathodic current at potentials less than about -0.2 V for $BaRuO_3$ in the presence of H_2O_2, and no changes above that potential. Compare with the large changes on Pt electrodes.

Finally, it should be noted that a large hysteresis in current was observed with all media when the scan was halted. On stopping the scan, the current rapidly fell toward zero. On restarting, the current returned rapidly to its initial value.

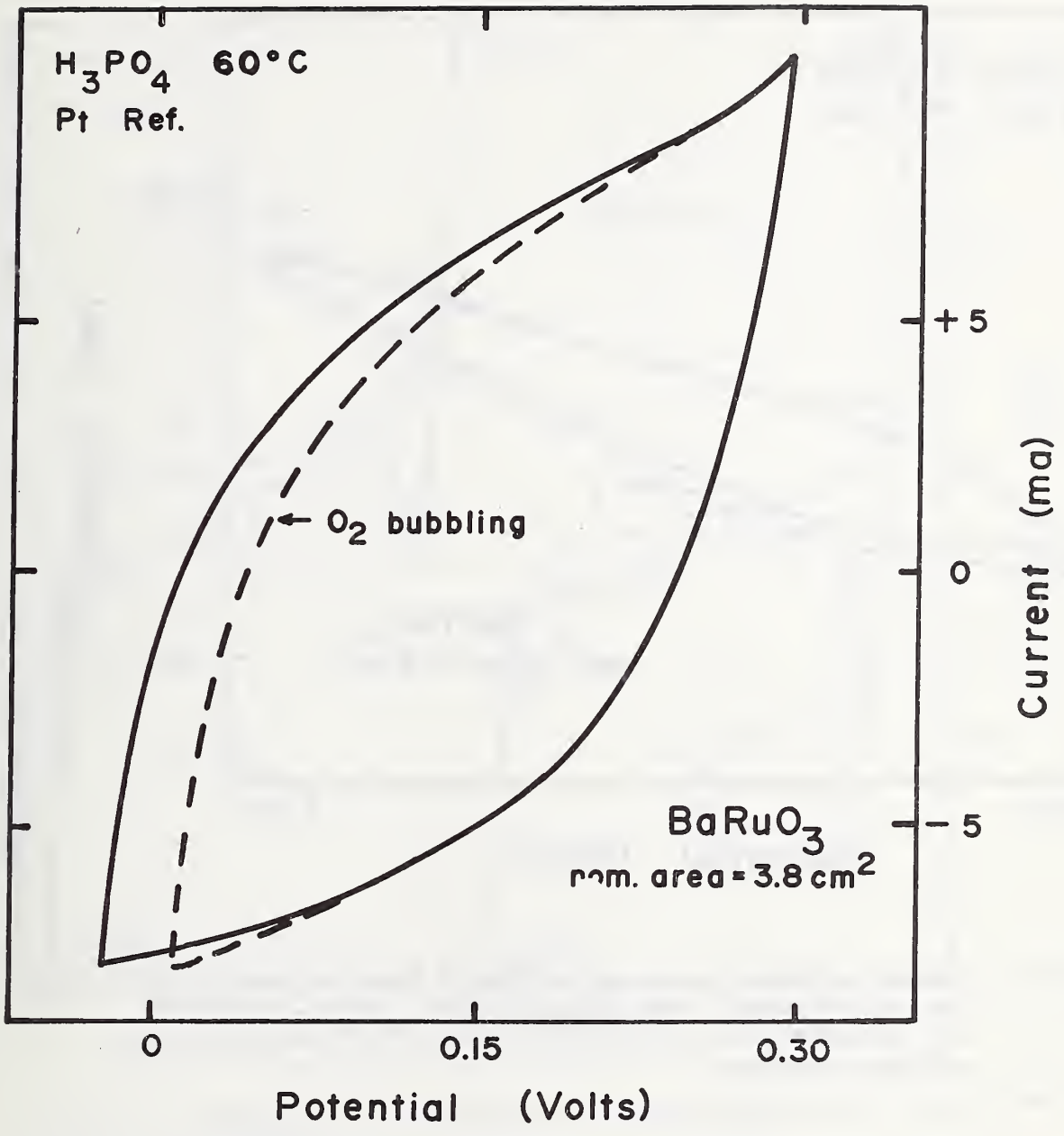

Figure 7. Effect of oxygen and the current-potential curve for a Type II $BaRuO_3$ electrode.

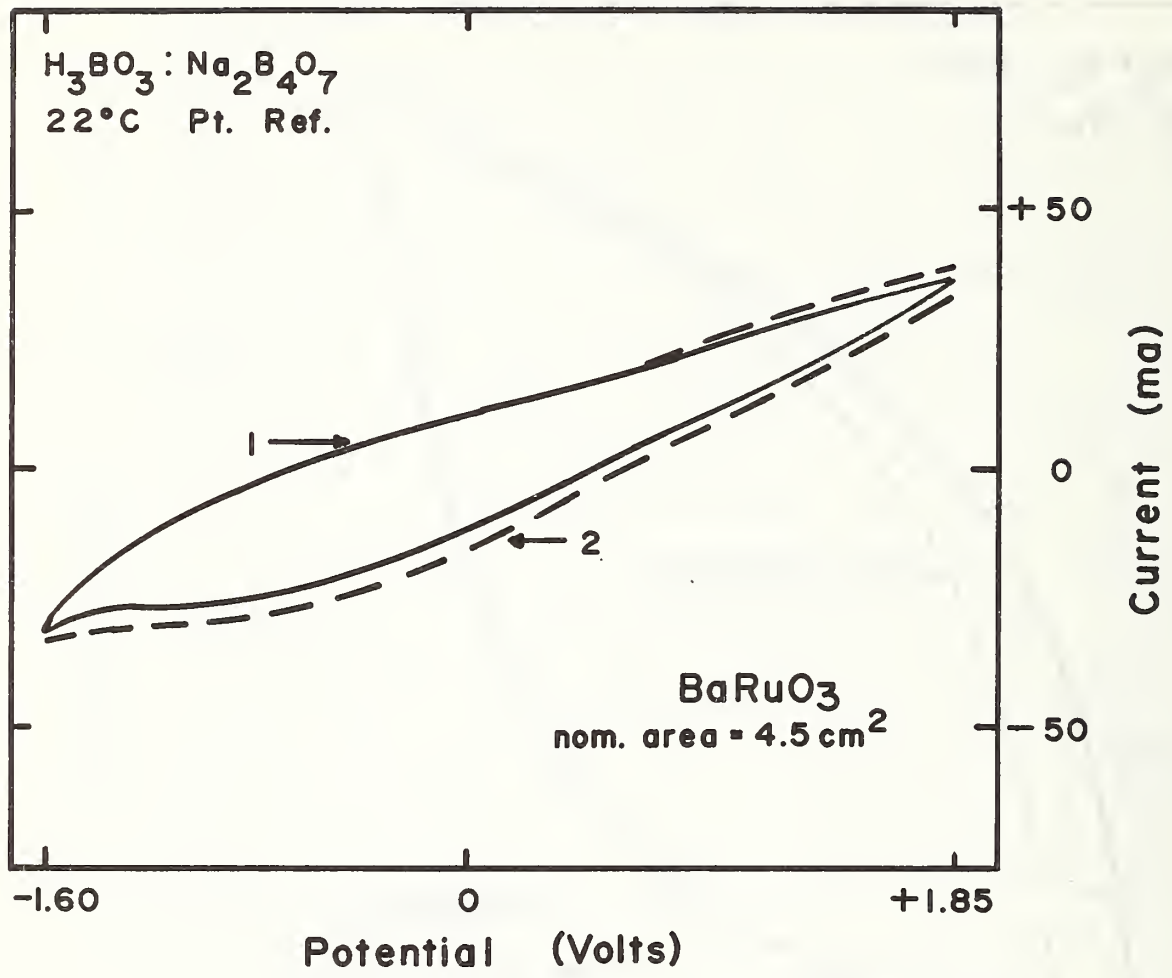

Figure 8. Current-potential curve for a Type II $BaRuO_3$ electrode in neutral solution. Scan range limited. Curve 1 is for an air saturated electrolyte. Curve 2 is for O_2 bubbling over electrode surface.

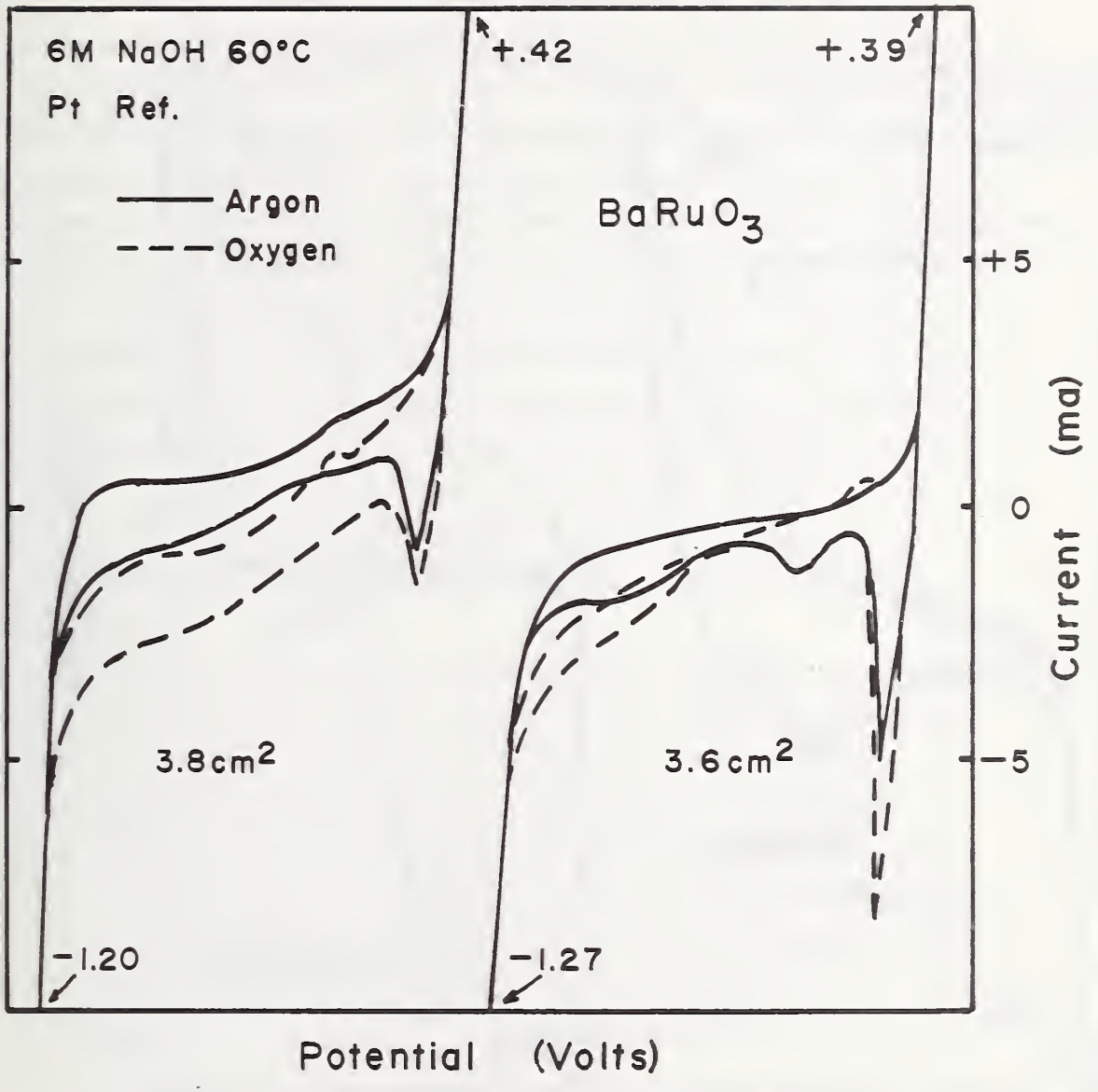

Figure 9. Comparison of two $BaRuO_3$ electrodes (Type II) in 6 mol/l (=M) NaOH at 60 °C.

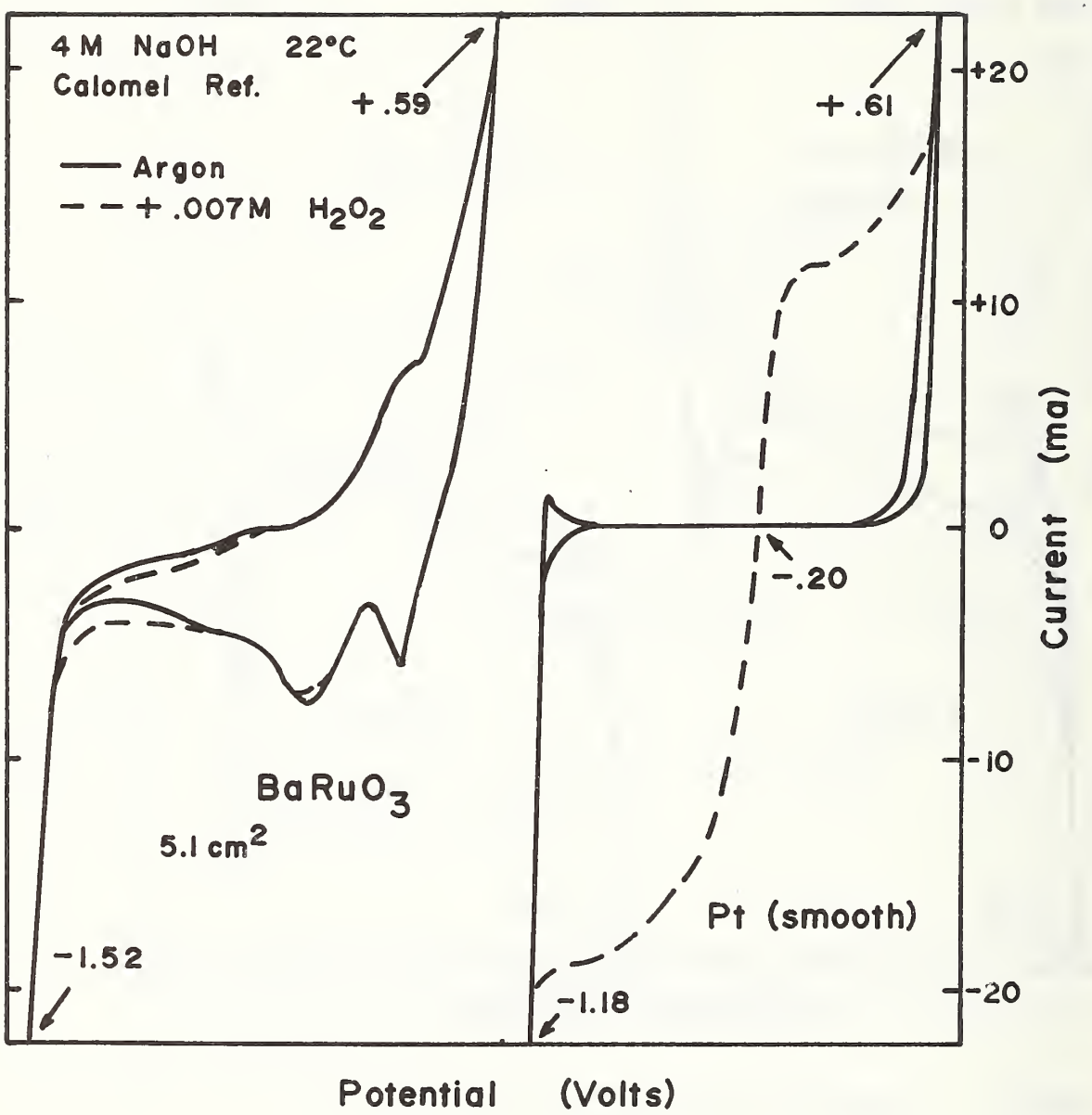

Figure 10. The effect of 0.007 M H_2O_2 on a Type II $BaRuO_3$ and on smooth Pt. M = mol/l.

Redox Measurements

In general, measurements of the performance of electrode materials with respect to single redox reactions were made in neutral solutions of 0.1 mol/l $K_3[Fe(CN)_6]$ + 0.1 mol/l $K_4[Fe(CN)_6]$, 0.1 mol/l $K_3[Fe(CN)_6]$ + 0.02 mol/l $K_4[Fe(CN)_6]$, and 0.1 mol/l KI_3 + 0.5 mol/l KI. Most of the measurements were carried out by potentiodynamic sweeping except in the cases of Type II $BaRuO_3$ electrodes, where, because of their porous nature, long times at constant current or voltage were required to attain steady state conditions.

In $K_3[Fe(CN)_6]/K_4[Fe(CN)_6]$ solutions for all electrodes tested, the open circuit potential corresponded to the equilibrium potential for the redox couple, so that the potential difference between the working electrode and the Pt reference electrode was at most a few millivolts. In KI/KI_3 solutions, however, the $SrTiO_3$ and TiO_2 electrodes tended to drift to -400 mV (vs. Pt) indicating that the potential was not determined by the I_3^-/I^- equilibrium.

With the exception of tungsten bronze in KI_3/KI, all materials were stable in these redox solutions. Some electrodes, however, showed increasing resistance with repeated anodic oxidation, indicating that the properties of the surface were changing, probably because of the formation of an insulating oxide layer. Larger currents could at times be restored by cathodic polarization to sufficiently negative potentials so that hydrogen evolution occurred. This behavior was seen with H_2 reduced TiO_2, 0.1% Nb doped TiO_2, $La_{0.75}Ca_{0.25}TiO_3$, and $La_{0.75}Sr_{0.25}TiO_3$.

Titanates -

For some of these materials a pronounced dissymmetry was observed, *i.e.*, the anodic currents were much smaller than the cathodic ones. Indeed, in some cases the rate of oxidation of $[Fe(CN)_6]^{4-}$ was negligible, as with $La_{0.75}TiO_3$ and $La_{0.92}TiO_3$.

Rutile (as grown) also exhibited similar dissymmetry, but the anodic current was larger. In contrast, a fairly symmetric current-potential curve was observed on Ta-doped TiO_2, as well as on two samples of $SrTiO_3$ with different amounts of Nb doping (0.03 and 0.15%).

At equal polarization, current densities varied considerably from material to material. To give an idea of their magnitude, exchange current densities very roughly estimated from $\Delta\eta/\Delta i$ (where η is the over-voltage) are reported in Table 2. In some cases, however, the dissymmetry is such that it is impossible to derive reliable values for the exchange current density.

Table 2. EXCHANGE CURRENT DENSITIES

Electrode	i_o (A/cm^2)	Behavior
TiO_3:5% Ta	10^{-7}	Symmetry
$SrTiO_3$:0.03% Nb	6×10^{-6}	Symmetry
$SrTiO_3$:0.15% Nb	2×10^{-6}	Symmetry
$La_{0.92}TiO_3$	2×10^{-9}	Dissymmetry
$La_{0.75}TiO_3$	7×10^{-8}	Dissymmetry
$La_{0.75}Ca_{0.25}TiO_3$	3×10^{-7}	Symmetry

None of the TiO_2 electrodes tested in KI_3/KI solution showed any detectable current (< 1μA) around the equilibrium potential, at least, from -300 to +700 mV. Nb doped $SrTiO_3$ showed no anodic current, and cathodic current only below -600 mV vs. Pt, and as already mentioned, anomalous behavior at open circuit.

Tungsten Bronze -

Tungsten bronze, $Na_{0.7}WO_3$ showed peculiar behavior. Around the equilibrium potential currents were large, but on the anodic side a limiting current of ∿ 8 mA at an over-voltage (η) of about 300 mV was reached. For polarizations higher than 0.6 V the current rapidly decreased to 500 μA or less (for η of the order of 1.2V) and further

increases in potential had no effect. It is unlikely that this behavior was due to chemical changes on the surface layers, but could have been due to the formation of a depletion layer. The exchange current density close to the equilibrium potential was fairly large, and can be estimated at about 4 mA/cm^2. This corresponds to a rate constant of 4×10^{-4} cm/sec, in good agreement with the values of Amjad and Pletcher[20] in acidified solution (0.4 mol/l H_2SO). As already mentioned, in KI_3/KI, the tungsten bronze dissolved; (the dissolution reaction seemed to occur in a regular fashion, leaving a flat and smooth surface). Because of this, the results are difficult to interpret, but they are consistent with the existence of a cathodic limiting current due to charge-carrier depletion on the electrode.

Barium Ruthenate -

Barium Ruthenate -

Steady-state data for a $BaRuO_3$-Type II electrode in two concentrations, 0.1M/0.1M and 0.1M/0.02M $K_3[Fe(CN)_6]/K_4[Fe(CN)_6]$, are reported in Figures 11 and 12, where M = mol/l. It is evident that a limiting current was reached on the cathodic side which was not due to transport in solution; (as a further indication, stirring had no effect on the limiting current). The effect was probably due to limited supply of charge-carriers in the electrode. The exchange current for the redox reaction was of the order of 500 μA for the first solution and 200 μA for the second. The current density cannot be established because the surface area is not known.

The behavior of $BaRuO_3$ with respect to the $[Fe(CN)_6]^{3-}/[Fe(CN)_6]^{4-}$ redox reaction is very interesting when compared with the behavior in a 0.1M KI_3/0.5M KI solution. The results, for the latter system, shown in Figure 13, indicate that on the cathodic side the limiting current was of the order of 3 to 4 mA, a value consistent with diffusion control. The current, therefore, was not limited by charge carrier supply on the electrode side.

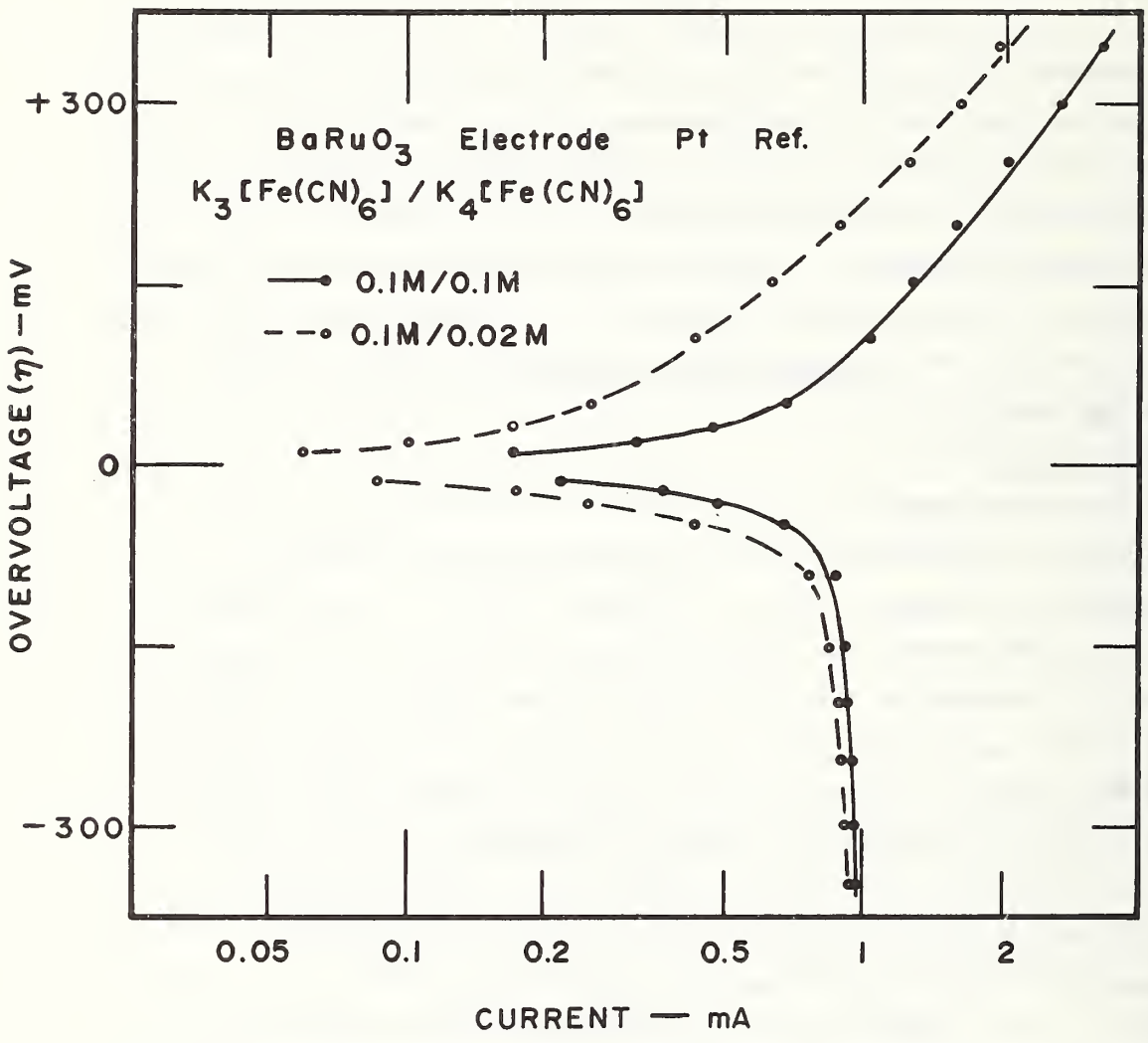

Figure 11. Ferro-ferricyanide reaction. Steady-state performance of Type II $BaRuO_3$ electrode. Plot of overvoltage versus logarithm of current. M = mol/l.

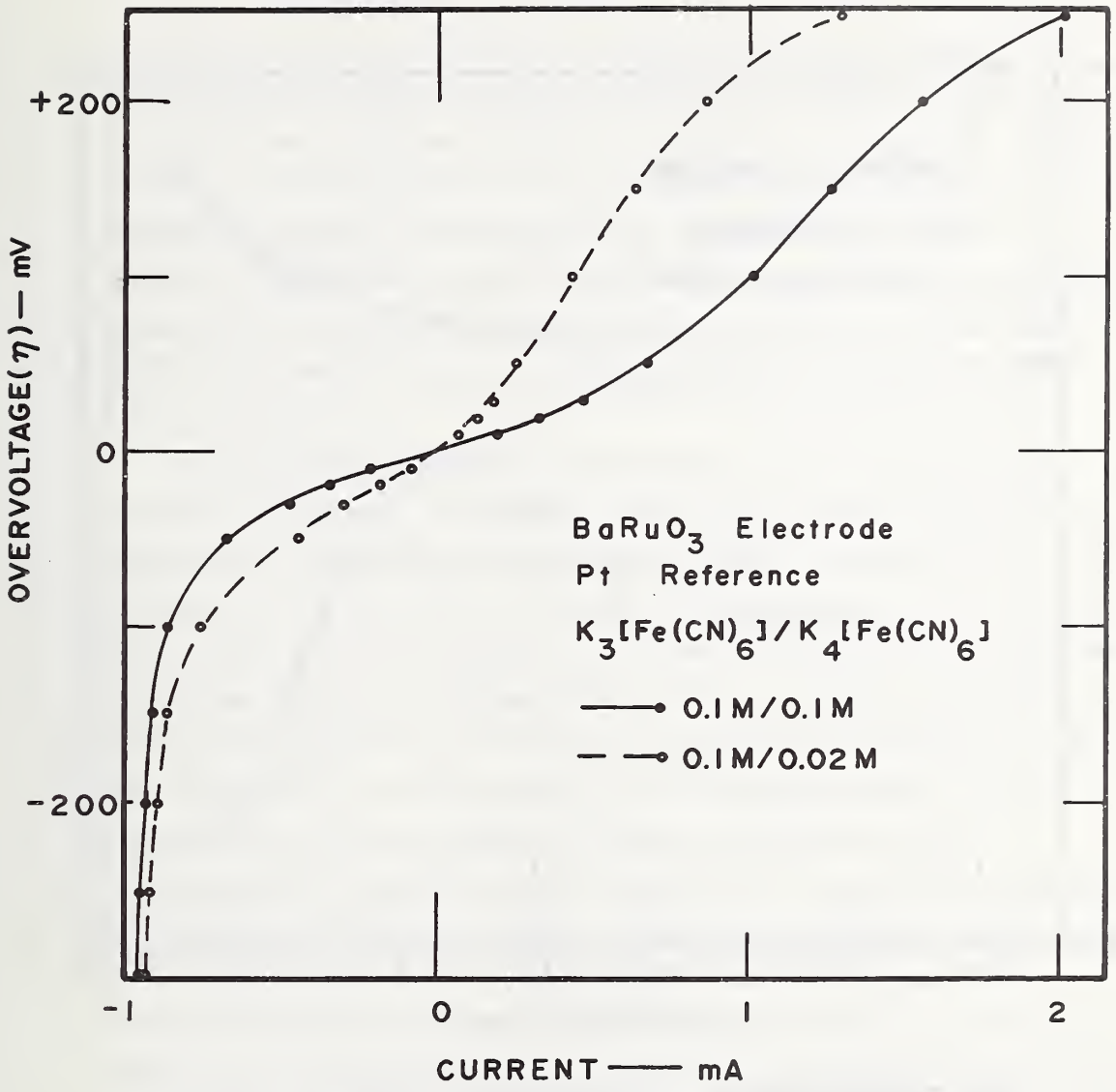

Figure 12. Ferro-ferricyanide reaction. Steady-state performance of Type II. $BaRuO_3$ electrode. Plot of overvoltage versus current. M = mol/l.

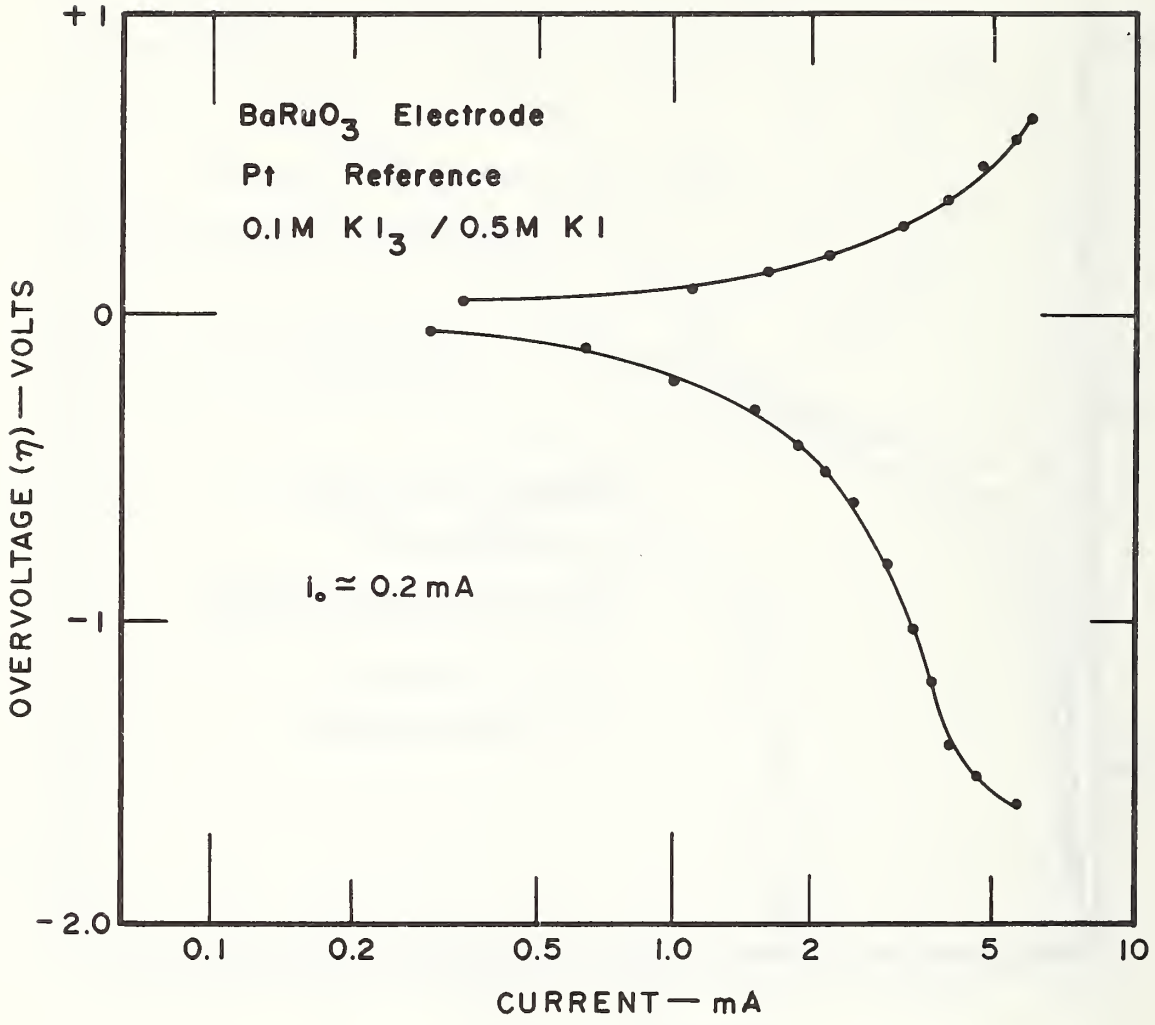

Figure 13. Iodine-iodide reaction. Steady-state performance of Type II $BaRuO_3$ electrode. Plot of overvoltage versus logarithm of current. M = mol/l.

DISCUSSION

The electrochemical measurements carried out to screen the materials for electrocatalytic properties have been perhaps more extensive than anticipated at the beginning of the contract, since less time than expected was used in readying the necessary instrumentation. Nevertheless, for the purpose of both forming a systematic picture of electrochemical behavior as related to chemical composition, and of investigating the reaction mechanisms occurring on non-metallic electrodes, the research done so far must be considered very preliminary, and few conclusions can be drawn at this point.

The following discussion, therefore, will be aimed at outlining a few general conclusions that emerge from the results, but even more at describing the research problems that have been uncovered, so as to help in directing future efforts in the field.

A first conclusion that can be drawn concerning experimental techniques is that electrodes produced from powders hot-pressed with binders tend to be porous with considerable disadvantages for the achievement of reliable data in a reasonable time: a large amount of the current observed on these electrodes during potentiodynamic scanning can be attributed to capacitative effects[21,22]. Even more troublesome than their long relaxation times is the difficulty of reproducible fabrication. For these reasons it is suggested that great effort be made to produce massive specimens as electrodes, and alternatively -- or better, concurrently -- to find methods to make electrodes from powders more reproducible and suitable for laboratory research.

As far as stability to hot, concentrated H_3PO_4 is concerned, a number of materials have shown increasing electrical resistance, that is, lower currents for the same scanning voltages particularly at more positive potentials. This indicates slow deterioration

of the surface properties, probably with formation of insulating oxides. These results point to the need to test for chemical stability under realistic polarization conditions.

Some of the materials tested, such as the various La titanates and $BaRuO_3$, exhibit metallic conductivity. However, in the electrochemical studies semiconducting properties have been observed. This is particularly evident in solutions containing redox couples, where, in many cases, the current tended to flow dissymmetrically in anodic and cathodic directions for reasons that appeared to be due to saturation of the charge-carrier current within the electrode.

Asymmetric behavior was also observed for some titanium oxide electrodes in phosphoric acid: on rutile (as grown) as well as 0.1% Nb doped TiO_2 no significant anodic current was detected. Whether this occurs because of surface depletion of electrons (these materials are n-semiconductors) or because of formation of an insulating phase is not clear. The situation is further confused since anodic current and oxygen evolution were obtained on 5% Ta doped TiO_2 and on H_2 reduced TiO_2, which are supposed to possess similar semiconducting characteristics.

As shown in Figure 5, the anodic behavior of the lanthanum titanates in H_3PO_4 seems to show an increase in anodic current with decreasing concentration of lanthanum, which corresponds to an increase in the valency of Ti from 3 (for $LaTiO_3$) to 4 (for $La_{0.67}TiO_3$. This could be attributed to a more pronounced n-semiconducting behavior for the more electron-rich titanate. However, if the effect is related to the formation of a depletion layer, the n-character appears to be a complicated function of composition, since the nominal valency of Ti is the same in $La_{0.92}TiO_3$ and in $La_{0.75}Ca_{0.25}TiO_3$, but the anodic current is larger on the latter. An alternative explanation might be based on a greater ease in forming an insulating layer (possibly TiO_2) by anodic oxidation in the case of lower valency titanate.

Most of the materials under investigation have also been tested as electrodes for two single redox reactions $K_3[Fe(CN)_6]/K_4[Fe(CN)_6]$ and KI_3/KI. The results obtained with $BaRuO_3$ and sodium tungsten bronze have been described in more detail and are quite interesting. Saturation currents are of opposite sign (cathodic for $BaRuO_3$ and anodic for $Na_{0.75}WO_3$). Since $BaRuO_3$ exhibits metallic conductivity, the semiconducting behavior might be explained by assuming that $BaRuO_3$ is a p-metal, and cathodic bias is sufficient to deplete holes at the surface. No saturation currents could be detected for $BaRuO_3$ in KI_3/KI. The reason might be linked to the equilibrium potential being more positive in KI_3/KI (+286 mV vs. SCE) compared with the ferri-ferrocyanide couple (+285 mV for the 0.1M/0.1M solution and +235 mV for the 0.1M/0.02M), but the differences in equilibrium potential seem rather small compared with the substantial (several tenths of a volt) polarizations applied, although it is not known how the potential difference is partitioned inside and outside the electrode.

The W bronze, which should tend to exhibit n-semiconductor properties, appeared to develop an exhaustion layer by anodic polarization in ferri-ferrocyanide, so that the current dropped by increasing bias. The other redox system used was not suitable since the bronze underwent dissolution, probably caused by hole injection on the part of the reducing iodine.

More redox systems have to be tested before a meaningful correlation with the oxygen reaction can be attempted, but it appears that materials on which little if any current can be drawn in H_3PO_4 exhibit similar behavior in ferri-ferrocyanide. The significance of the behavior in KI_3/KI is much more confused, since for many of the materials tested even the equilibrium potential is not determined by the I^{3-}/I^- equilibrium and no current is obtained.

SECTION VII

MATERIALS OTHER THAN OXIDES

INTRODUCTION

In agreement with molecular orbital theory, the reduction of oxygen is easy and that of nitrogen difficult. Biochemical reduction of nitrogen, however, takes place under mild conditions, the final product being ammonia. The ordering of molecular orbitals in nitrogen and oxygen is very similar, leading to the expectation that similarities between the reduction of oxygen and nitrogen may exist, and that the nitrogen reductase enzyme (nitrogenase) might serve as a useful model for compounds capable of catalyzing the reduction of oxygen at electrode surfaces. The active site of nitrogenase consists of a molybdenum-nonheme iron-sulfur array in which molybdenum is thought to be involved in the final electron transfer steps. In order to pursue this analogy further, the synthesis of ternary metal sulfide arrays, in which one of the metals is molybdenum or tungsten, was undertaken with a view to providing an alternative approach to the central thrust of this program.

RESULTS

1. Aqueous Systems. Metathetical reactions in water, *e.g.*,

$$Fe^{++} + MoS_4^{2-} \longrightarrow FeMoS_4$$

failed and the products were ferrous sulfide and molybdenum disulfide. Analogous reactions were attempted with dithiotungstate(2-), $WO_2S_2^{2-}$, in the hope that the transition metal oxythiotungstates would be more stable. However, unusual solvolysis reactions supervened and sulfur-free products were isolated, *e.g.*,

$$Cr^{+++} + WO_2S_2^{2-} \longrightarrow Cr_2(WO_4)_3 \cdot 3H_2O$$

A publication describing these results is in press. In order to avoid complications introduced by reactions with water, nonaqueous syntheses were studied.

2. Nonaqueous Sytems. In order to solubilize transition metal ions in organic solvents, it is usually necessary to employ large, hydrophobic ligands. Triphenylphosphine was chosen for use in initial experiments, primarily because of its ready availability. Use of tertiary phosphines confers another potential advantage, for these ligands are often labile. Thus dissociation in solution of the phosphine may uncover a coordination site on a metal atom to produce a species, in equilibrium concentration, too reactive to be isolated.

A simple metathetical reaction between $(Ph_3P)_3CuCl$ and $(Ph_3PCH_3)_2WO_2S_2$ in dichloromethane was attempted. The product, $(Ph_3P)_4Cu_2W_2S_6$, isolated by chromatography on silica gel, was oxygen-free. This suggested that triphenylphosphine could serve as a reducing agent to remove oxygen and sulfur from $WO_2S_2^{2-}$ to produce the desired ternary metal sulfides; the by-products are Ph_3PO and Ph_3PS.

This copper-tungsten-sulfur complex has been studied by a variety of physical techniques and some of its physical properties are tabulated below:

yellow-orange crystalline solid, soluble in chlorinated hydrocarbons

mp. 227-230° (dec.) (under vacuum)

$\{^1H\}^{31}P$ NMR: broad singlet at -8.1 ppm from H_3PO_4

^1H NMR: complex multiplet centered at -7.5 ppm

IR: 448 cm^{-1} (ν_{ws})

Raman: 467(s), 254(w)

Electronic spectrum: λ_{max} at 440, 267 nm

E_p(oxidation) - 1.14 V; E_p(reduction) - 0.94, - 1.5 V (vs. SCE, irreversible; by cyclic voltametry).

The general synthetic route (metal ion, triphenylphosphine, and $WO_2S_2^{2-}$) has been extended to other coinage metals. The Ag-W-S system has proved to be particularly instructive. The

initial product is a yellow solid whose elemental analysis corresponds to $(Ph_3P)_6Ag_5W_2S_6O_2$. Attempts to further purify this product led to its decomposition into a mixture of an orange and a yellow material. The elemental analysis of the yellow material, separated by fractional crystallization, corresponds to $[(Ph_3P)_3Ag]_2W_2S_6$. It is converted on boiling in dichloromethane-acetone to the orange material, whose analysis corresponds to $(Ph_3P)_3Ag_3WS_3$. It is possible that the orange compound is not a single phase and this question is being pursued. These observations suggest that the initial product in the Ag-Ph_3P-$WO_2S_2^{2-}$ system is a complex oxythiotungstate which undergoes further reaction on the acidic sites on silica gel to form a W_2S_6 complex.

Using Ph_3PAuCl as the starting material, the only product isolated was $(Ph_3PAu)_2W_2S_4$. Like the related copper complex, this material had a molecular weight half that of the expected value, suggesting that the phosphine ligands are indeed labile. Only in the case of gold was a new product formed when triphenylarsine was used as a reducing agent. It appears to be a simple tetrathiatungstate(2-) derivative, $(Ph_3AsAu)_2WS_4$.

The physical techniques employed to date do not provide an adequate structural characterization of these ternary metal sulfides, which are new and quite novel materials, and x-ray diffraction studies are needed. The triphenylphosphine complexes generally have low molar solubilities, making it difficult to grow crystals and those that are obtained are usually thin flakes. Preparation of tri-p-tolylphosphine and diphenylmethylphosphine analogues is currently underway. Good single crystals of the diphenylmethylphosphine-gold-tungsten sulfide have been obtained. They are monoclinic with a = 15.46 Å, b = 13.51 Å, and β = 96°. An x-ray study of this material has just begun. Some single crystals of orange $(Ph_3P)_3Ag_3WS_3$ have also been grown and cell parameters are now being measured. These more soluble derivatives

will be useful for studies of ^{31}P NMR spectra, since the triphenylphosphine complexes are so poorly soluble that exhorbitant amounts of spectrometer time are required to obtain even marginal data.

Materials characterization has now proceeded sufficiently far that applications in real systems can be considered. Arrangements have been made for fabrication of composite electrodes containing $(Ph_3P)_4Cu_2W_2S_2$ and graphite. These will be examined in a working cell to test for catalytic activity in oxygen reduction.

A limited effort has been made to prepare ternary arrays containing nickel, palladium, or platinum. Metathesis between $WO_2S_2^{2-}$ and (diphos)$NiCl_2$ is straightforward and (diphos)$NiWO_2S_2$ is produced. This material appears to be a mixture of geometric isomers. Similar reactions with (diphos)$PdCl_2$ and *cis*-$(Ph_3P)_2PtCl_2$ led to $(diphos)_2Pd_3W_2S_6O_2$ and $(Ph_3P)_3PtW_2S_6O_2$. These yellow microcrystalline materials are virtually insoluble in nonreactive solvents and their characterization is extremely difficult [diphos = 1,2-*bis*(diphenylphosphino)ethane].

SECTION VIII

REFERENCES

1. Gillis, A. E. Advanced Development. In: Seventh Status Report on Fuel Cells, Huff, J. R. (ed.). U. S. Army Mobility Equipment Research and Development Center, Fort Belvoir, Va. Report 2039. NTIS No. AD-755 106. October 1972. 174 p.
2. Negas, T., and R. S. Roth. J. Solid State Chem. 1:409-418, 1970.
3. Negas, T., and R. S. Roth. J. Solid State Chem. 3:323-339, 1971.
4. Negas, T. J. Solid State Chem. 6:136-150, 1973.
5. Negas, T., and R. S. Roth. Proceedings of 5th Materials Research Symposium, National Bureau of Standards, Washington, D.C. NBS Special Publication No. 364. July 1972. 31 p.
6. Candela, G. A., A. H. Kahn, and T. Negas. J. Solid State Chem. 7:360-369, 1973.
7. Negas, T. J. Solid State Chem. 7:85-88, 1973.
8. Kestigian, M., and R. Ward. J. Am. Chem. Soc. 77:6199-6200, 1955.
9. Donohue, P. C., L. Katz, and R. Ward. Inorg. Chem. 4:306-310, 1965.
10. Callaghan, A., C. W. Moeller, and R. Ward. Inorg. Chem. 5:1573-1576, 1966.
11. Bouchard, R. J., and J. L. Gillson. Mat. Res. Bull. 7:873-878, 1972.
12. Waring, J. L., and R. S. Roth. J. Res. NBS. 27A:175-186, 1968.
13. Waring, J. L., and R. S. Roth. J. Res. NBS. 69A:119-129, 1965.
14. Nicks, L. J., and D. J. MacDonald. Report of Investigations 7841, U. S. Department of Interior, Bureau of Mines, Washington, D.C. 1973. 9 p.

15. Bodiot, D. Revue de Chemie Minerale. 5:569-607, 1968.

16. Graham, J. Am. Mineral. 59:1045-1046, 1974.

17. Stern, M., and A. C. Makrides. J. Electrochem. Soc. 107:782, 1960.

18. Neidrach, L. W., and H. R. Alford. J. Electrochem. Soc. 112:117-124, 1965.

19. O'Grady, W., C. Iwakura, J. Huang, and E. Yenger. Ruthenium Oxide Catalysts for the Oxygen Electrode. ONR Technical Report 37, Case Western Reserve, Cleveland, Ohio. 1974. 22 p.

20. Amjad, M., and D. Pletcher. Electroanalytical Chem. and Interfacial Electrochem. 59:61-67, 1975.

21. Austin, L. G., and E. G. Gagnon. J. Electrochem. Soc. 120:251-254, 1973.

22. Gagnon, E. G. J. Electrochem. Soc. 120:1052-1056, 1973; *Ibid*. 121,512-515, 1974; *Ibid*., 122:521-525, 1975.

SECTION IX

LIST OF PUBLICATIONS

1. Siedle, A. R., T. Negas, and J. Broussalian. "Reaction of Transition Metal Ions with the Dithiotungstate(2-) Ion." J. Inorg. Nucl. Chem. In press.

NBS-114A (REV. 7-73)

U.S. DEPT. OF COMM. BIBLIOGRAPHIC DATA SHEET	1. PUBLICATION OR REPORT NO. NBSIR 75-742	2. Gov't Accession No.	3. Recipient's Accession No.

4. TITLE AND SUBTITLE

MIXED OXIDES FOR FUEL CELL ELECTRODES

5. Publication Date: January 1976

6. Performing Organization Code

7. AUTHOR(S) U. Bertocci, M. Cohen, W. S. Horton, T. Negas, and A. R. Siedle

8. Performing Organ. Report No.

9. PERFORMING ORGANIZATION NAME AND ADDRESS

NATIONAL BUREAU OF STANDARDS
DEPARTMENT OF COMMERCE
WASHINGTON, D.C. 20234

10. Project/Task/Work Unit No. 3130402

11. Contract/Grant No. EPA-IAG D4-0528

12. Sponsoring Organization Name and Complete Address *(Street, City, State, ZIP)*

EPA, Office of Research and Development
Industrial Environmental Research Laboratory
Research Triangle Park, NC 27711

13. Type of Report & Period Covered: Final: 5/74-5/75

14. Sponsoring Agency Code

15. SUPPLEMENTARY NOTES

EPA Report No: EPA-600-2-76-007

16. ABSTRACT *(A 200-word or less factual summary of most significant information. If document includes a significant bibliography or literature survey, mention it here.)*

Studies of mixed oxides were made in order to determine if such materials could act as oxygen-reducing electrocatalysts in an acid fuel cell. Included were strontium and barium cobaltates and manganates with and without added titanium; lanthanum titanates, with and without calcium or strontium; calcium, strontium, and barium ruthenates; and mixed oxides of the systems Ti-Ta-O, V-Nb-O, Ce-Ta-O, Pr-Ta-O, Ce-Nb-O, and Ce-Pr-Ta-O. Choices were based upon producing variable valence and upon conferrring stability at elevated temperatures ($\lesssim$ 150 °C) in phosphoric acid. Barium ruthenate and the systems Ti-Ta-O, V-Nb-O, V-Ta-O, Ce-Ta-O were hot-acid stable. The thermal reactions of $CeTaO_{4+x}$ with $0 \lesssim x \lesssim 0.5$ were studied in air up to about 1960 °C.

Potentiodynamic and galvanostatic studies are reported on materials from the Ti-Ta-O system, TiO_2 as grown, TiO_2 reduced with hydrogen, TiO_2 with 0.1% Nb, lanthanum titanates with and without calcium or strontium, a tungsten bronze, barium ruthenate, and strontium titanate with .03% and with .15% Nb.

Preparation of inorganic compounds with ternary metal-sulfur arrays similar to the arrays in nitrogen reductase was attempted. The following were made: $(Ph_3P)_4Cu_2W_2S_6$, $(Ph_3P)_6Ag_5W_2S_6O_2$, and $[(Ph_3P)_3Ag]_2W_2S_6$, where Ph_3P refers to the triphenylphosphine moiety. Also prepared were $(Ph_3PAu)_2W_2S_4$, $(Ph_3AsAu)_2WS_4$, $(diphos)NiWO_2S_2$, $(diphos)_2Pd_3W_2S_6O_2$, and $(Ph_3P)_3PtW_2S_6O_2$, where "diphos" refers to 1,2-bis(diphenylphosphino)ethane.

17. KEY WORDS *(six to twelve entries; alphabetical order; capitalize only the first letter of the first key word unless a proper name; separated by semicolons)*

Electrocatalysis; fuel cells; mixed oxides, oxygen reduction; phosphoric acid; ternary metal-sulfur arrays; transition elements; triphenylphosphine; tungsten bronze

18. AVAILABILITY [XX] Unlimited

[ ] For Official Distribution. Do Not Release to NTIS

[ ] Order From Sup. of Doc., U.S. Government Printing Office Washington, D.C. 20402, SD Cat. No. C13

[ ] Order From National Technical Information Service (NTIS) Springfield, Virginia 22151

19. SECURITY CLASS (THIS REPORT): UNCLASSIFIED

21. NO. OF PAGES: 57

20. SECURITY CLASS (THIS PAGE): UNCLASSIFIED

22. Price

USCOMM-DC 29042-P74